Atmos. Chem. Phys. Discuss., https://doi.org/10.5194/acp-2017-597
Manuscript under review for journal Atmos. Chem. Phys.
Discussion started: 24 October 2017

Atmospheric Chemistry and Physics Discussions

Impacts of Aerosols on Seasonal Precipitation and Snowpack in California Based on Convection-Permitting WRF-Chem Simulations

Longtao Wu[1], Yu Gu[2], Jonathan H. Jiang[1], Hui Su[1], Nanpeng Yu[3], Chun Zhao[4], Yun Qian[5], Bin Zhao[2], Kuo-Nan Liou[2], and Yong-Sang Choi[1,6]

[1]*Jet Propulsion Laboratory, California Institute of Technology, Pasadena, CA, USA.*

[2]*Joint Institute for Regional Earth System Science and Engineering and Department of Atmospheric and Oceanic Science, University of California, Los Angeles, CA, USA*

[3]*Department of Electrical and Computer Engineering, University of California, Riverside, Riverside, CA, USA*

[4]*School of Earth and Space Sciences, University of Science and Technology of China, Hefei, Anhui, China*

[5]*Atmospheric Sciences and Global Change Division, Pacific Northwest National Laboratory, Richland, WA, USA*

[6]*Department of Environmental Science and Engineering, Ewha Womans University, Seoul, South Korea*

Atmos. Chem. Phys. Discuss., https://doi.org/10.5194/acp-2017-597
Manuscript under review for journal Atmos. Chem. Phys.
Discussion started: 24 October 2017

Atmospheric Chemistry and Physics Discussions

Highlights:

1. Aerosols warm the California mountain tops through aerosol-snow interaction by local dust but cools the lower elevation areas through aerosol-radiation interaction and aerosol-cloud interaction by transported and local anthropogenic aerosols.
2. Aerosols reduce precipitation and snowpack in California primarily through aerosol-cloud interaction by transported and local anthropogenic aerosols and aerosol-snow interaction by local dust.
3. Aerosols cause earlier snowmelt at mountain tops through aerosol-snow interaction by local dust, leading to reduced surface runoff after April.

Atmos. Chem. Phys. Discuss., https://doi.org/10.5194/acp-2017-597
Manuscript under review for journal Atmos. Chem. Phys.
Discussion started: 24 October 2017

Atmospheric Chemistry and Physics Discussions

Abstract

A version of the WRF-Chem model with fully coupled aerosol-meteorology-snowpack is employed to investigate the impacts of various aerosol sources on precipitation and snowpack in California. In particular, the impacts of locally emitted anthropogenic and dust aerosols, and aerosols transported from outside of California are studied. We differentiate three pathways of aerosol effects including aerosol-radiation interaction (ARI), aerosol-snow interaction (ASI), and aerosol-cloud interaction (ACI). The convection-permitting model simulations show that precipitation, snow water equivalent (SWE), and surface air temperature averaged over the whole domain (34-42°N, 117-124°W, not including ocean points) are reduced when aerosols are included, therefore reducing the high model biases of these variables when aerosol effects are not considered. Aerosols affect California water resources through the warming of mountain tops and anomalously low precipitation, however, different aerosol sources play different roles in changing surface temperature, precipitation and snowpack in California by means of various weights of the three pathways. ARI by all aerosols mainly cools the surface, leading to slightly increased SWE over the mountains. Locally emitted dust aerosols warm the surface of mountain tops through ASI, in which the reduced snow albedo associated with dirty snow leads to more surface absorption of solar radiation and reduced SWE. Transported and local anthropogenic aerosols play a dominant role in increasing cloud water amount but reducing precipitation through ACI, leading to reduced SWE and runoff over the Sierra Nevada, as well as the warming of mountain tops associated with decreased SWE and hence lower surface albedo. The average changes in surface temperature from October to June are about −0.19 K and 0.22 K for the whole domain and over mountain tops, respectively. Overall, the averaged reduction during October to June is about 7% for precipitation, 3% for SWE, and 7% for surface runoff for the whole domain,

53 while the corresponding numbers are 12%, 10%, and 10% for mountain tops. The reduction in
54 SWE is more significant in a dry year, with 9% for the whole domain and 16% for mountain tops.
55 The maximum reduction of ~20% in precipitation occurs in May associated with the maximum
56 of aerosol loadings, leading to the largest decrease in SWE and surface runoff over that time
57 period. It is also found that dust aerosols could cause early snowmelt at the mountain tops and
58 reduced surface runoff after April.
59
60 **1. Introduction**
61 Water resources in California are derived predominantly from precipitation (mostly during
62 the winter time) and storage in the snowpack in the Sierra Nevada. Snowpack provides about
63 one-third of the water used by California's cities and farms. The fresh water stored in the
64 snowpack gradually releases through runoff into river flows during the warm and dry season.
65 The amount and timing of snowmelt are critical factors in determining water resources in this
66 region. It is important to understand the factors influencing precipitation and snowpack on
67 seasonal timescale for water management and hydropower operation.
68 The 2012-2014 California drought has been attributed to both warming and anomalously
69 low precipitation (Griffin and Anchukaitis, 2014). Previous studies have suggested that warming
70 trends are amplified in mountains compared to lowlands because of the moist adiabatic structure
71 of the atmosphere and snow-albedo feedback (Leung et al., 2004). In addition to the warming
72 effects of greenhouse gases, aerosols may have substantial impacts on water resources in
73 California. Recent observational and numerical modeling studies have shown that aerosol
74 pollutants can substantially change precipitation and snowpack in California (e.g., Rosenfeld et
75 al., 2008a; Qian et al., 2009a; Hadley et al., 2010; Ault et al., 2011; Creamean et al., 2013, 2015;

Fan et al., 2014; Oaida et al., 2015). Lee and Liou (2012) illustrated that approximately 26% of snow albedo reduction from March to April over the Sierra Nevada is caused by an increase in aerosol optical depth (AOD).

In California, aerosols can be generated locally or transported from remote sources. Among local aerosol types, dust comprises a significant fraction over California (Wu et al., 2017). Based on a four-month, high intensity record of size-segregated particulate matter (PM) samples collected from a high elevation site, Vicars and Sickman (2011) found that the mass concentration of coarse atmospheric PM in the southern Sierra Nevada, California, was dominated by contribution from dust (50-80%) throughout the study period. Dust aerosols can exert important impact on radiative forcing and regional climate in California through its interaction with radiation (e.g., Zhao et al., 2013a) as well as its role as cloud condensations nuclei for cloud formation (e.g., Fan et al., 2014). Anthropogenic aerosols are geographically distributed because of localized emission sources and the short atmospheric residence time. The anthropogenic aerosols can cause changes in atmospheric circulation and regional climate especially where the aerosol concentrations are high and the synoptic atmospheric systems are not prominent (e.g., Qian et al., 2003; Fast et al., 2006; Rosenfeld et al., 2008a; Zhao et al., 2013a).

Besides the local aerosol sources, the atmospheric transport of aerosol pollutants from the Asian continent (e.g., Jiang et al., 2007; Wang et al., 2015; Hu et al., 2016) is also a significant contributor to aerosol loading throughout the Pacific basin. Asian aerosols can reach relatively high concentrations above the marine boundary layer in the western US, representing as much as 85% of the total atmospheric burden of PM at some sites (VanCuren, 2003). Trans-Pacific dust transport has been found to be particularly relevant in high-elevation regions such as the Sierra

Nevada, which typically represents free-tropospheric conditions due to the limited transport of lowland air pollutants and predominance of upper air subsidence (VanCuren et al., 2005). Observations from the CalWater campaign demonstrated that dust and biological aerosols transported from northern Asia and the Sahara were present in glaciated high-altitude clouds in the Sierra Nevada coincident with elevated ice nuclei (IN) particle concentrations and ice-induced precipitation (Ault et al., 2011; Creamean et al., 2013).

Aerosols can influence precipitation, snowpack and regional climate through three pathways: (1) aerosol-radiation interaction (ARI, also known as aerosol direct effect), which can warm the atmosphere but cool the surface, resulting in changes in thermodynamic environment for cloud and precipitation and the delay of the snowmelt (Charlson et al., 1992; Kiehl and Briegleb, 1993; Hansen et al., 1997; Koren et al., 2004; Gu et al., 2006, 2016, 2017); (2) aerosol-cloud interaction (ACI, also known as aerosol indirect effect), which is related to aerosols serving as cloud condensation nuclei (CCN) and IN. By changing the size distribution of cloud droplets and ice particles, aerosol may affect cloud microphysics, radiative properties and precipitation efficiency, thus affect the atmospheric hydrological cycle and energy balance (Twomey, 1977; Jiang and Feingold, 2006; Rosenfeld et al., 2008b; Qian et al., 2009b; Gu et al., 2012); (3) aerosol-snow interaction (ASI). When aerosols (mainly absorbing aerosols, such as dust and black carbon) are deposited on snow, they can reduce snow albedo and affect snowmelt (Warren and Wiscombe, 1985; Jacobson, 2004; Flanner et al., 2007; Qian et al., 2011, 2015; Zhao et al., 2014). Numerical experiments have shown that ARI reduces the surface downward radiation fluxes, cools the surface and warms the atmosphere over California (Kim et al., 2006; Zhao et al., 2013a), which could subsequently impact clouds, precipitation and snowpack. In a 2-D simulation, Lynn et al. (2007) shows that ACI decreases orographic precipitation by 30% over

the length of the mountain slope. Fan et al. (2014) showed that ACI increases the accumulated precipitation of an Atmospheric River event by 10-20% from the Central Valley to the Sierra Nevada due to a ~40% increase in snow formation. Snow impurities (ASI) increase ground temperature, decrease snow water, shorten snow duration and cause earlier runoff (Jacobson, 2004; Painter et al., 2007, 2010; Qian et al., 2009a; Waliser et al., 2011; Oaida et al., 2015).

Although recent studies showed that aerosols can substantially influence precipitation and snowpack in California, they focused only on one of the aerosol sources or on a single event or one pathway. A complete account of the aerosol impacts from different sources through three pathways on regional climate in California has not been presented yet. The objective of this study is to investigate the impacts of various aerosol sources on seasonal precipitation and snowpack in California. A fully coupled high-resolution aerosol-meteorology-snowpack model will be used. We will distinguish and quantify the impacts of aerosols from local emissions and transport, and the roles of different prevailing aerosol types in California, particularly dust and anthropogenic aerosols. In Section 2, we describe the WRF-Chem model employed and experiments designed to understand the impact of aerosols on precipitation and snowpack in California. Results from model simulations are discussed in Section 3. Concluding remarks are given in Section 4.

2. Model Description and Experiment Design

This study uses a version of the Weather Research and Forecasting (WRF) model with chemistry (WRF-Chem; Grell et al., 2005) improved by the University of Science and Technology of China (USTC) based on the public-released version 3.5.1 (Zhao et al., 2014). ASI is implemented in this WRF-Chem version by considering aerosol deposition on snow and the

subsequent radiative impacts through the SNow, ICe, and Aerosol Radiative (SNICAR) model (Zhao et al., 2014). The SNICAR model is a multilayer model that accounts for vertically heterogeneous snow properties and heating and influence of the ground underlying snow (Flanner and Zender, 2005; Flanner et al., 2007, 2009, 2012). The SNICAR model uses the theory from Wiscombe and Warren (1980) and the two-stream, multilayer radiative approximation of Toon et al. (1989). SNICAR simulates snow surface albedo as well as the radiative absorption within each snow layer. It can also simulate aerosol content and radiative effect in snow, and was first used to study the aerosol heating and snow aging in a global climate model by Flanner et al. (2007). Simulated change of snow albedo by SNICAR for a given black carbon concentration in snow has been validated with recent laboratory and field measurements (Brandt et al., 2011; Hadley and Kirchstetter, 2012). More detailed description of the SNICAR model can be found in Flanner and Zender (2005) and Flanner et al. (2007, 2012).

The MOSAIC (Model for Simulating Aerosol Interactions and Chemistry) aerosol model (Zaveri et al., 2008) with the CBM-Z (carbon bond mechanism) photochemical mechanism (Zaveri and Peters, 1999) is used and coupled with the SNICAR model. The MOSAIC aerosol scheme uses the sectional approach to represent aerosol size distributions with a number of discrete size bins, either four or eight bins in the current version of WRF-Chem (Fast et al., 2006). In this study, aerosol particles are partitioned into four-sectional bins with dry diameter within 0.039-0.156 μm, 0.156-0.625 μm, 0.625-2.5 μm, and 2.5-10.0 μm. The 4-bin approach has been examined in dust simulations and proved to reasonably produce dust mass loading and AOD compared with the 8-bin approach (Zhao et al., 2013b). All major aerosol components including sulfate, nitrate, ammonium, black carbon, organic matter, sea salt, and mineral dust are simulated in the model. The MOSAIC aerosol scheme includes physical and chemical processes

of nucleation, condensation, coagulation, aqueous phase chemistry, and water uptake by aerosols. Dry deposition of aerosol mass and number is simulated following the approach of Binkowski and Shankar (1995), which includes both particle diffusion and gravitational effects. Wet removal of aerosols by grid resolved stratiform clouds/precipitation includes in-cloud removal (rainout) and below-cloud removal (washout) by impaction and interception, following Easter et al. (2004) and Chapman et al. (2009). In this study, cloud-ice-borne aerosols are not explicitly treated in the model but the removal of aerosols by the droplet freezing process is considered. Aerosol optical properties such as extinction, single scattering albedo (SSA), and asymmetry factor for scattering are computed as a function of wavelength for each model grid box. Aerosols are assumed internally mixed in each bin, i.e., a complex refractive index is calculated by volume averaging for each bin for each chemical constituent of aerosols (Barnard et al., 2010; Zhao et al., 2013a). The Optical Properties of Aerosols and Clouds (OPAC) data set (Hess et al., 1998) is used for the shortwave (SW) and longwave (LW) refractive indices of aerosols, except that a constant value of 1.53+0.003i is used for the SW refractive index of dust following Zhao et al. (2010, 2011). A detailed description of the computation of aerosol optical properties in WRF-Chem can be found in Fast et al. (2006) and Barnard et al. (2010).

The model setups (Table 1), including the physical schemes used, follow Wu et al. (2017), which showed that the model simulations reasonably captured the distribution and variation of aerosols in the San Joaquin Valley. Note that convective processes are resolved in the 4 km simulations. ARI is included in the radiation scheme as implemented by Zhao et al. (2011). The optical properties and direct radiative forcing of individual aerosol species in the atmosphere are diagnosed following the methodology described in Zhao et al. (2013a). Calculation of the activation and re-suspension between dry aerosols and cloud droplets was included in the model

by Gustafson et al. (2007). By linking simulated cloud droplet number with shortwave radiation and microphysics schemes, ACI is effectively simulated in the model (Chapman et al., 2009).

The model domain covers the Western US centered at 38°N and 121°W, as shown in Fig. 1. The horizontal resolution is 4 km × 4 km together with a vertical resolution of 40 model levels. Model integrations have been performed for 10 months (with the first month used for the model spin-up) starting on September 1, 2012, at 00:00UTC till the end of June 2013 to cover the major precipitation and snow seasons. Simulations have also been done for year 2013-2014, and similar results are found. In the following result section, our analysis focuses on year 2012-2013, while quantitative information of aerosol impacts for year 2013-2014 is provided for comparison. To examine the overall aerosol effects and the roles of locally generated and transported aerosols, the following five experiments have been designed (Table 2):

1) CTRL: This is the control experiment with all aerosol emissions and transports included in the simulation.

2) NoDust: This experiment is performed without any local dust emission. Differences between the CTRL and NoDust experiments illustrate the effect of dust aerosols locally emitted.

3) NoAnth: This experiment is similar to NoDust, except that emissions of local anthropogenic aerosols are turned off. Comparison between CTRL and this experiment will elucidate the effect of local anthropogenic aerosols.

4) NoTran: In this experiment, aerosol transport from outside the model domain is not considered by setting the lateral boundary conditions for aerosols to zero. Differences between CTRL and this experiment will show the effect of transported aerosols.

5) CLEAN: This experiment is performed without any local aerosol emissions or transport from outside the model domain, and therefore represents a scenario of clean condition.

Differences between the CTRL and CLEAN experiments would illustrate the effects of all primary aerosol types, including those locally emitted and transported from outside the domain.

In order to distinguish the pathways through which the aerosols influence the precipitation and snowpack, we also conducted a few other experiments (Table 3):

6) NARI: This experiment is similar to the CTRL, except that ARI is not included. Comparison between CTRL and this experiment will elucidate the effect of ARI.

7) NASI: This experiment is similar to the CTRL, except that ASI is not included. Comparison between CTRL and this experiment will show the effect of ASI.

8) NARS: In this experiment, both ARI and ASI are not included. By comparing this experiment and CLEAN, the effect due to ACI can be examined.

3. Model Simulation Results

3.1 Validation of Model Results

Since our focus is on changes in precipitation and snowpack due to aerosol effects, we first show the spatial distribution of averaged results over the period from October to June when snow normally presents over the Sierra Nevada. Figure 2 illustrates a few important and relevant variables that the model simulates in CTRL experiment, including liquid water path (LWP), ice water path (IWP), precipitation, snow water equivalent (SWE), and temperature at two meters (T2) above the ground. It is shown that clouds (Figs. 2a & 2b), precipitation (Fig. 2c) and snow (Fig. 2d) mostly occur over the Sierra Nevada and Klamath Mountains in the northern California. For temperature (Fig. 2e), the central valley area appears to be relatively warm with two maxima over the northern and southern part of the central valley, respectively, while colder temperature is found over the mountain ranges. The model-simulated precipitation is compared with

237 corresponding observations from the Climate Prediction Center (CPC) Unified Gauge-Based
238 Analysis of Daily Precipitation product at 0.25° × 0.25° resolution (Fig. 2f). Compared to CPC
239 observations, the model successfully captures the precipitation pattern, including the locations of
240 the major precipitation centers, but overestimates the magnitude over the Sierra Nevada.

241 In order to validate the simulated seasonal variations, the monthly mean model simulated
242 precipitation and T2 are compared with observations (Figs. 3a & 3c). For precipitation
243 observations, besides the CPC product, we also employ the measurements from Department of
244 Water Resources (DWR). Observed air temperature is obtained from the California Irrigation
245 Management Information System (CIMIS; http://www.cimis.water.ca.gov/). For SWE, daily
246 mean SWE simulations are compared with measurements collected at Snow Telemetry
247 (SNOTEL) stations. The use of the SNOTEL data, including known deficiencies, has been
248 described in several studies (e.g., Serreze et al., 1999; Serreze et al., 2001; Johnson and Marks,
249 2004). The main issue with weighing-type gauges for snowfall estimation is the undercatch of
250 approximately 10%–15% due to wind (Serreze et al., 2001; Yang et al., 1998; Rasmussen et al.,
251 2001). Model data are sampled onto observational sites before the comparison is conducted. It is
252 shown that the model captures the maximum precipitation in December, with the magnitude
253 falling between the observations from CPC and DWR during winter, which is the major rainy
254 season in California (Fig. 3a). For SWE, given the possible underestimate of SNOTEL data, the
255 model simulations represent reasonable magnitude and seasonal variations with the maximum
256 between March and April (Fig. 3b). While the model overestimates the surface temperature in
257 magnitude, it captures the seasonal variations well, including the highest/lowest temperature in
258 July/January, respectively (Fig. 3c). Therefore, the WRF-Chem model that we employ in this

study is a reliable tool for examining the impact of aerosols on the seasonal variations of precipitation and snowpack in California, especially over the Sierra Nevada.

The simulated aerosols over California using this model have been validated extensively in Wu et al. (2017) by comparing to observations, such as MISR (Multiangle Imaging Spectroradiometer) and AERONET (Aerosol Robotic Network) AOD, CALIPSO (Cloud-Aerosol Lidar and Infrared pathfinder Satellite Observation) aerosol extinction, IMPROVE (Interagency Monitoring of Protected Visual Environments) and EPA CSN (National Chemical Speciation Network operated by Environmental Protection Agency) aerosol speciation. It has been shown than the model simulation used in this study reasonably captures the distribution and seasonal variation in aerosols during the cold season from October to March. The simulation of aerosols in the warm season from April to September (especially from July to September) has larger low biases than in the cold season, mainly due to poor simulations of dust emission and vertical mixing. Because the precipitation and snow mainly occurs in October-June, we focus on the simulations from October to June with relative good performance on aerosol simulations in this study.

Here, we present the distributions of locally emitted aerosols and those transported from outside the model domain together with the total aerosols from the CTRL experiment in Fig. 4 to facilitate the understanding of the aerosol effects in different regions and from different sources. It is shown that the maximum of total AOD is located over the southern part of the valley area. Larger AODs are also found over the lower lands to the southeast of the Sierra Nevada. The distribution of the locally emitted anthropogenic aerosols (Fig. 4b), which are mostly located over the central valley associated with the emissions from local industries and farms, presents a similar pattern to the total AOD and substantially contributes to the maxima AOD over the

region. Local dust aerosols mainly reside over the lower lands to the southeast of the Sierra Nevada (Fig. 4c). Transported aerosols, including dust and biological aerosols from East Asia (Creamean et al., 2013), are carried into the domain by atmospheric circulation and widely distributed, with more over the central valley due to the trapping of aerosols by the surrounding mountains (Fig. 4d).

3.2 Aerosol Effects on Precipitation and Snowpack

The overall aerosol effects, from all aerosol types and sources (including locally emitted and transported) through the three pathways (ARI, ACI, and ASI), can be examined from the differences between the experiments CTRL and CLEAN. Figure 5 shows the differences in precipitation, SWE, and T2, where the dots represent differences of the daily data being statistically significant at above 90% level. Due to the aerosol effects, temperature decreases over the central valley, where most aerosols are located, while significant warming occurs over the mountain tops (Fig. 5c). Precipitation decreases over the Sierra Nevada (Fig. 5a), consequently leading to decreased SWE (Fig. 5b).

In order to understand how the aerosols affect these important variables, we examine the effects of ARI, ACI, and ASI separately. It is seen that the major effect of ARI is to decrease the surface temperature over the whole domain through the scattering and absorption of solar radiation, with the maxima over the central valley where the aerosols are mostly located, contributing to the surface cooling caused by the total aerosols effects in that region (Fig. 6c). The ARI induced surface cooling over the Sierra Nevada, although not as strong as over the central valley, leads to reduced snowmelt and hence slight increase in SWE, opposite to the overall aerosol effect on SWE (Fig. 6b). The effect of ARI on rainfall is not very significant (Fig.

305 6a). The main effect of ASI is to increase the temperature (Fig. 7c) over the snowy area of the
306 Sierra Nevada through the reduction of snow albedo (Fig. 7d) and hence more absorption of solar
307 radiation at the surface, contributing to the reduced SWE over the Sierra (Fig. 7b). The effect of
308 ASI on precipitation is also minimal.

309 Figure 8 shows the effect of aerosols on clouds through ACI. When more aerosols are
310 present in the atmosphere, more cloud condensation nuclei (CCN) are available for the formation
311 of clouds with smaller cloud droplets. As a result, more non-precipitating clouds are produced
312 when aerosol are included in the model. The enhanced LWP (Fig. 8a) is primarily produced by
313 the ACI effect (Fig. 8c). There are no significant changes in IWP (including ice, snow, and
314 graupel) because aerosol effect on ice cloud formation is not explicitly treated in the model. The
315 ACI effect leads to reduced precipitation and less SWE over the mountains (Figs. 9a & 9b).
316 Temperature decreases over the valley due to more clouds formed associated with ACI effect.
317 Note that the negative differences shown here (Fig. 9c) are only significant at 70% level. The
318 increase in temperature over the mountain areas (Fig. 9c) is caused by the reduced snow amount,
319 which results in weaker surface albedo (Fig. 9d) and enhanced solar absorption at the surface.

320 Overall, aerosols affect surface temperature, precipitation, and snowpack in California
321 through the three pathways. ACI plays a dominant role in increasing cloud water but reducing
322 precipitation, leading to reduced SWE and runoff over the Sierra Nevada. ASI also reduces SWE
323 due to the smaller snow albedo associated with dirty snow, leading to more surface absorption
324 and snowmelt. ARI, on the other hand, slightly increases SWE through the cooling of surface.
325 For surface temperature, ARI and ACI contribute together to the cooling of the valley area, while
326 ACI and ASI significantly warm the surface over the mountain tops. Note that for ASI effect,
327 warming of the snow cover area through aerosol-snow albedo feedback is the cause for the

reduced SWE. For ACI effect, however, warming over the mountain region is a result from the reduced SWE and hence smaller surface albedo and more surface absorption of solar radiation.

Next, we examine the roles of local anthropogenic aerosols and dust as well as transported aerosols. The effect of local anthropogenic aerosols can be discovered from the differences between CTRL and NoAnth. It is shown that local anthropogenic aerosols slightly suppresses the rainfall (Fig. 10a) via ACI, leading to reduced SWE (Fig. 10b) and a warming over the mountain tops (Fig. 10c). The cooling of the valley area, where locally emitted anthropogenic aerosols are mostly located (Fig. 4b), is associated with both the ARI effect and more clouds produced through ACI. Dust aerosols emitted from local sources mainly warm the surface through the reduction of snow albedo (ASI, Fig. 11c), consequently enhancing the snowmelt and leading to reduced SWE (Fig. 11b). Local dust aerosols, mostly generated from the area to the southeast of Sierra Nevada, do not seem to have significant effect on precipitation (Fig. 11a).

Note that the effects of local anthropogenic and dust aerosols do not seem to be able to explain the total effects of aerosols as seen in Fig. 5, raising the question whether the transported aerosols play an important role in the precipitation and snowpack over the Sierra Nevada. Figure 12 illustrates the impact of aerosols transported from outside the model domain. It is shown that transported aerosols also reduce the precipitation through ACI (Fig. 12a), leading to decreased SWE and increased temperature over the southern part of Sierra Nevada (Figs. 12b & 12c). Due to the ARI effect of the transported aerosols, temperature decreases over the central valley, as well as over the northern part of the Sierra (Fig. 12c), resulting in less snowmelt and increased SWE over that region (Fig. 12b).

The overall changes induced by aerosols for surface temperature (K) and precipitation, SWE, and surface runoff in percentage averaged over October to June are given in Table 4 for

351 the whole domain (34-42 °N, 117-124 °W, not including ocean points), mountain tops (elevation
352 ≥ 2.5 km), and lower elevations (elevation < 2.5 km). For the whole domain in year 2012-2013,
353 temperature is cooled by 0.19 K due to aerosol ARI (−0.14 K), as well as ACI (−0.06 K) mainly
354 associated with transported aerosols (−0.17 K), accompanied by reduction in precipitation, SWE,
355 and surface runoff of about 7%, 3%, and 7%, respectively. Reduction in precipitation is mainly
356 caused by ACI (−6.26%) associated with transported (−2.97%) and local anthropogenic (−1.02%)
357 aerosols. For SWE, reduction is attributed to ACI (−2.67%) and ASI (−1.96%), while ARI
358 contributes to the increase (1.88%). Changes in surface runoff are similar to those in
359 precipitation. For the mountain tops, warming of 0.22 K is found attributed to ASI (0.12 K) and
360 ACI (0.17 K) associated with dust and anthropogenic aerosol, respectively, with 10% or more
361 reduction in the precipitation, snowpack, and surface runoff. Therefore, aerosols may contribute
362 to California drought through both the warming of mountain tops and anomalously low
363 precipitation over the whole area. For the lower elevations, the domain averaged changes are
364 similar to those for the whole domain, except for SWE which slightly increases by 0.42% due to
365 ARI (2.43%) with main contribution from transported aerosols (4.01%).

366 The simulations for year 2013-2014 are consistent with those in year 2012-2013 (Table 4).
367 For the whole domain in year 2013-2014, temperature is cooled by 0.21 K due to aerosols,
368 accompanied by reduction in precipitation, SWE, and surface runoff of about 6%, 9%, and 5%,
369 respectively. Aerosol impacts on SWE is more significant in year 2013-2014 (−8.88%) than in
370 year 2012-2013 (−3.17%), possibly due to less precipitation and SWE in year 2013-2014 than
371 year 2012-2013 (not shown). The changes of SWE for year 2013-2014 are −15.57% for the
372 mountain tops and 2.66% for the lower elevations. The change of surface runoff at the mountain

tops in year 2013-2014 is smaller than year 2012-2013, possibly contributed by less SWE at the mountain tops in year 2013-2014.

3.3 Seasonal Variations of Aerosol Effects

Figure 13 depicts the monthly mean AOD for total aerosols (brown solid), local anthropocentric aerosols (green dashed), local dust (blue dashed), and transported aerosols (red dashed) averaged over the whole domain, the mountain tops, and lower elevation area from October 2012 to June 2013. It is seen that transported aerosols contribute to about two-thirds of the total AOD. The total AOD has two maxima, one in December and one in May, mainly associated with the seasonal variations of transported aerosols and dust aerosols. Dust AOD starts to increase in March and reaches a maximum around May, while transported aerosol AOD peaks in April (Fig. 13a). The seasonal variations of AOD over the mountain tops and lower elevations are similar to those of the whole domain (Figs. 13b & 13c).

The monthly mean differences in precipitation due to the total aerosols (brown solid), ARI (green solid), ASI (blue solid), ACI (red solid), local anthropocentric aerosols (green dashed), local dust (blue dashed), and transported aerosols (red dashed) are shown in Fig. 14. Reduced precipitation is seen over the whole domain, with the most contribution from transported aerosols, followed by anthropogenic aerosols, both of which play roles in precipitation changes through ACI as previously shown. ARI, ASI, or locally emitted dust aerosols do not seem to play an important role in the monthly mean precipitation changes (Fig. 14a). Two maxima of aerosol effects are found: one in December when it is the rainy season of the California (Fig. 3a) and at the same time relatively larger AOD presents over the region (Fig. 13a); the other peak reduction in precipitation due to the aerosol effects is found in May with a value of about 0.2 mm day^{-1}

(Fig. 13a), probably associated with the maximum aerosols (Fig. 13a) and also the precipitation over the mountain region due to orographic forcing over that time period (Lee et al. 2015). Given that the monthly mean precipitation in May is only about 1 mm day^{-1} (Fig. 3a), the reduction caused by aerosols is about 20%. For monthly mean precipitation, changes over the mountain tops and the lower elevation area, respectively, have similar seasonal variation patterns (Figs. 14b & 14c).

For SWE, however, changes over the mountain tops are different from those in the lower area (Fig. 15). For mountain tops, negative changes in SWE are seen over the whole time period, with a maximum reduction of about 60 mm in May corresponding to the maximum AOD (Fig. 15b). Major contribution is from dust aerosols through ASI, as well as transported and anthropogenic aerosols through ACI. ARI produces small positive changes (~ 5 mm in May) in SWE due to the scattering and absorption of solar radiation by aerosols which leads to surface cooling. For lower elevation area, slightly enhanced SWE is found during winter time, associated with the effects of transported aerosols which produce more clouds through ACI, and together with the ARI effect, lead to the cooling of the surface and hence less snowmelt. (Fig. 15c). Over the whole domain, SWE is reduced with a maximum of about 2 mm in May, equivalent to about 2% reduction, mainly attributed to the dust particles through ASI, and anthropogenic and transported aerosols through ACI (Fig. 15a).

Changes in temperature also exhibit different patterns over the mountain tops and the lower elevations (Fig. 16). Warming over the mountain tops is produced by dust aerosols through ASI with a maximum around May, and by transported aerosols through ACI during winter which leads to reduced precipitation and SWE with a maximum in January (Fig. 16b). Cooling over the lower elevation areas is caused by ARI, and also induced by more clouds generated in model

419 simulations due to transported aerosols through ACI, with a maximum cooling of about 0.3 K in
420 April, corresponding to the maximum AOD of transported aerosols (Fig. 16c). The average
421 temperature changes over the whole domain are negative because of the large area of the lower
422 elevations (Fig. 16a).

423 Surface runoff is defined as water from rain, snowmelt, or other sources that flows over the
424 land surface, and is a major component of the hydrological cycle. Surface runoff is mainly
425 associated with precipitation and the changes present a similar pattern to those in precipitation
426 for the whole domain (Fig. 17a) and lower elevation areas (Fig. 17c), with most contribution
427 from transported and anthropogenic aerosols. For the mountain tops, surface runoff shows a
428 slight increase in spring, and then a decrease after April (Fig. 17b). The increase can be
429 explained by the effect of dust aerosols deposited on the snow, which reduces the snow albedo
430 through ASI and warms the surface, leading to more and earlier snowmelt than normal. The
431 decrease after April is a combined effect of earlier snowmelt due to dust aerosols and reduced
432 precipitation caused by transported and anthropogenic aerosols through ACI. Thus, the impact of
433 aerosols is to speed up snowmelt at mountain tops.
434

435 **4. Conclusions**

436 A fully coupled high-resolution aerosol-meteorology-snowpack model is employed to
437 investigate the impacts of various aerosol sources on precipitation and snowpack in California.
438 The relative roles of locally emitted anthropogenic and dust aerosols, and aerosols transported
439 from outside of the domain are differentiated through the three pathways, aerosol-radiation
440 interaction, aerosol-snow interaction, and aerosol-cloud interaction.

441 **Temperature**: Dust aerosols warm the mountain top surfaces through ASI (0.12 K), in
442 which the reduced snow albedo associated with dirty snow leads to more surface absorption of
443 solar radiation. Transported and local anthropogenic aerosols warm the surface of mountain tops
444 through ACI (0.17 K), which produces more clouds but reduces precipitation and hence snow
445 amount, leading to decreased surface albedo and more absorption of solar energy. The cooling of
446 the valley area (–0.21 K) is primarily caused by the scattering and absorption of all aerosols
447 through ARI (–0.14 K). Transported and anthropogenic aerosols can also cool the surface over
448 the central valley through ACI (–0.07 K) that enhances cloud amount, leading to more reflection
449 of solar radiation.

450 **Precipitation and SWE**: Reduced precipitation of –6.87% is found due to the aerosol
451 effects and is mainly caused by transported and local anthropogenic aerosols through ACI
452 (–6.26%). The maximum of aerosol effect on precipitation is found in December during the rainy
453 season when the aerosols loadings are also relatively large. The other peak effect occurs in May
454 with a reduction of about 20%, probably associated with the maximum of aerosol loadings and
455 more orographic precipitation over the mountains. Locally emitted dust aerosols represent one of
456 the most important contributors to the reduced SWE (–3.17%) through ASI (–1.96%), with the
457 largest reduction in May corresponding to the maximum dust emission over that time.
458 Anthropogenic aerosols can also reduce SWE through ACI (–2.67%). On the other hand, ARI
459 (2.43%) by all aerosols, with most contributions from the transported aerosols, exceeds the
460 effects of ASI (–0.99%) and ACI (–0.27%) and slightly enhance SWE by 0.42% over lower
461 elevations in winter time through the surface cooling.

462 **Surface runoff**: As a major component of the water cycle, surface runoff is mainly
463 generated by precipitation. We find that the surface runoff is reduced by –6.58% associated with

suppressed precipitation, caused by transported and anthropogenic aerosols through ACI (–6.30%). Over mountain tops, runoff slightly increases in spring due to the enhanced solar absorption by dust aerosols. Runoff decreases after April as a combined effect of earlier snowmelt due to dust and reduced precipitation due to transported and anthropogenic aerosols through ACI. Therefore, one of the important impacts of aerosols is to speed up the snowmelt at mountain tops.

In summary, we find that the WRF-Chem model simulations with aerosol effects included would produce lower precipitation and SWE by about 10% and colder temperature by 0.2 K over California than the simulations without aerosols. Therefore, including aerosol effects can reduce the high biases of these variables in the simulations reported previously. Aerosols play an important role in California water resources through the warming of mountain tops and the subsequent modification of precipitation and snowmelt. The total aerosol effects produce a warming of 0.22 K over mountain tops and a reduction from October to June in precipitation, SWE, and surface runoff of about 7%, 3%, and 7%, respectively, for the whole domain, with corresponding numbers of 10% or more over mountain tops. In a dry year (year 2013-2014), aerosol can have more significant impacts on SWE, with a reduction of up to 9% for the whole domain and 16% over mountain tops.

It is still quite challenging to accurately represent aerosol properties in the model (Fast et al., 2014). As pointed out by Wu et al. (2017), biases exist in the current model as compared to observations, for example, underestimation of AOD due to poor representation of dust emission and vertical mixing in the warm season. Given the importance role that dust plays in the California snowpack, improved dust emission and vertical mixing are needed for accurate quantification of the impact of dust. Also, the underestimation of organic matter (associated with

secondary organic aerosol processes) in the model (Wu et al., 2017), which are primarily scattering aerosols, would contribute to the high bias in the simulation of surface temperature. More accurate representation and simulation of these aerosols in the model are needed. Our results are based on two years of simulations. Additional simulations under different meteorological conditions will help to better assess the aerosol impacts on California hydrology quantitatively.

Data availability

The CPC data are available through the following link: https://www.esrl.noaa.gov/psd/data/gridded/data.unified. The CIMIS data are available through the following link: http://wwwcimis.water.ca.gov/. The SNOTEL data are available through the following link: https://www.wcc.nrcs.usda.gov/snow/.

Competing interests

The authors declare that they have no conflict of interest.

Acknowledgements

This study was carried out at the Joint Institute for Regional Earth System Science and Engineering and Department of Atmospheric and Oceanic Science, University of California, Los Angeles, and sponsored by California Energy Commission under grant #EPC-14-064. LW, JHJ, HS, and YSC conducted the work at the Jet Propulsion Laboratory, California Institute of Technology, under contract with the National Aeronautics and Space Administration. They acknowledge the funding support from the NASA ACMAP program. CZ is supported by the

510 "Thousand Talents Plan for Young Professionals" program of China. The contribution of YQ is
511 supported by the U.S. Department of Energy (DOE), Office of Science, Biological and
512 Environmental Research as part of the Regional and Global Climate Modeling Program. The
513 Pacific Northwest National Laboratory (PNNL) is operated for DOE by Battelle Memorial
514 Institute under contract DE-AC05-76RL01830.

515

516 References

517 Ault, A. P., Williams, C. R., White, A. B., Neiman, P. J., Creamean, J. M., Gaston, C. J., Ralph,
518 F. M., and Prather K. A.: Detection of Asian dust in California orographic precipitation, J.
519 Geophys. Res., 116, D16205, doi:10.1029/2010JD015351, 2011.
520 Binkowski, F. S. and Shankar, U.: The Regional Particulate Matter Model: 1. Model description
521 and preliminary results, J. Geophys. Res., 100: doi: 10.1029/95JD02093. issn: 0148-0227,
522 1995.
523 Bishop, J. K. B., Davis, R. E., and Sherman J. T.: Robotic observations of dust storm
524 enhancement of carbon biomass in the North Pacific, Science, 298, 817–821,
525 doi:10.1126/science.1074961, 2002.
526 Barnard, J. C., Fast, J. D., Paredes-Miranda, G., Arnott, W. P., and Laskin, A.: Technical Note:
527 Evaluation of the WRF-Chem "Aerosol Chemical to Aerosol Optical Properties" Module
528 using data from the MILAGRO campaign, Atmos. Chem. Phys., 10, 7325–7340,
529 doi:10.5194/acp-10-7325-2010, 2010.
530 Brandt, R. E., Warren, S. G., and Clarke, A. D.: A controlled snowmaking experiment testing the
531 relation between black-carbon content and reduction of snow albedo, J. Geophys. Res. 116,
532 D08109, 2011.

533 Chadwick, O. A., Derry, L. A., Vitousek, P. M., Huebert, B. J., and Hedin L. O.: Changing
534 sources of nutrients during four million years of ecosystem development, Nature, 397, 491–
535 497, doi:10.1038/17276, 1999.
536 Charlson, R. J., Schwartz, S. E., Hales, J. H., Cess, R. D., Coakley Jr., J. A., Hansen, J. E., and
537 Hofmann D. J.: Climate forcing by anthropogenic aerosols, Science, 255, 423–430,
538 doi:10.1126/science.255.5043.423, 1992.
539 Chapman, E. G., Gustafson Jr., W. I., Easter, R. C., Barnard, J. C., Ghan, S. J., Pekour, M. S.,
540 and Fast, J. D.: Coupling aerosolcloud-radiative processes in the WRF-Chem model:
541 Investigating the radiative impact of elevated point sources, Atmos. Chem. Phys., 9, 945–
542 964, doi:10.5194/acp-9-945-2009, 2009.
543 Creamean, J. M., Suski, K. J., Rosenfeld, D., Cazorla, A., DeMott, P. J., Sullivan, R. C., White,
544 A. B., Ralph, F. M., and Prather, K. A.: Dust and biological aerosols from the Sahara and
545 Asia influence precipitation in the western US, Science, 339(6127), 1572–1578,
546 doi:10.1126/science.1227279, 2013.
547 Creamean, J. M., Ault, A. P., White, A. B., Neiman, P. J., Ralph, F. M., Minnis, P., and Prather,
548 K. A.: Impact of interannual variations in sources of insoluble aerosol species on
549 orographic precipitation over California's central Sierra Nevada, Atmos. Chem. Phys., 15,
550 6535-6548, doi:10.5194/acp-15-6535-2015, 2015.
551 Durkee, P. A., Chartier, R. E., Brown, A., Trehubenko, E. J., Rogerson, S. D., Skupniewicz, C.,
552 Nielsen, K. E., Plantnick, S, and King, M. D.: Composite ship track characteristics, J.
553 Atmos. Sci., 57, 2542-2553, 2000.
554 Easter, R. C., et al.: MIRAGE: Model description and evaluation of aerosols and trace gasses. J.
555 Geophys. Res., 109, D20210, doi:10.1029/ 2004JD004571, 2004.

556 Fan, J., Leung, L. R., DeMott, P. J., Comstock, J. M., Singh, B., Rosenfeld, D., Tomlinson, J. M.,
557 White, A., Prather, K. A., Minnis, P., Ayers, J. K., and Min, Q.: Aerosol impacts on
558 California winter clouds and precipitation during CalWater 2011: local pollution versus
559 long-range transported dust, Atmos. Chem. Phys., 14, 81-101, doi:10.5194/acp-14-81-2014,
560 2014.
561 Fast, J. D., Gustafson Jr., W. I., Easter, R. C., Zaveri, R. A., Barnard, J. C., Chapman, E. G.,
562 Grell, G. A. and Peckham, S. E.: Evolution of ozone, particulates, and aerosol direct
563 radiative forcing in the vicinity of Houston using a fully coupled meteorology-chemistry-
564 aerosol model, J. Geophys. Res., 111, D21305, doi:10.1029/2005JD006721, 2006.
565 Fast, J. D., Allan, J., Bahreini, R., Craven, J., Emmons, L., Ferrare, R., Hayes, P. L., Hodzic, A.,
566 Holloway, J., Hostetler, C., Jimenez, J. L., Jonsson, H., Liu, S., Liu, Y., Metcalf, A.,
567 Middlebrook, A., Nowak, J., Pekour, M., Perring, A., Russell, L., Sedlacek, A., Seinfeld, J.,
568 Setyan, A., Shilling, J., Shrivastava, M., Springston, S., Song, C., Subramanian, R., Taylor,
569 J. W., Vinoj, V., Yang, Q., Zaveri, R. A., and Zhang, Q.: Modeling regional aerosol and
570 aerosol precursor variability over California and its sensitivity to emissions and long-range
571 transport during the 2010 CalNex and CARES campaigns, Atmos. Chem. Phys., 14, 10013-
572 10060, doi:10.5194/acp-14-10013-2014, 2014.
573 Flanner, M. G., and Zender, C. S.: Snowpack radiative heating: Influence on Tibetan Plateau
574 climate, Geophys. Res. Lett., 32, L06501, doi:10.1029/2004GL022076, 2005.
575 Flanner, M. G., Zender, C. S., Randerson, J. T., and Rasch, P. J.: Present-day climate forcing and
576 response from black carbon in snow, J. Geophys. Res., 112, D11202,
577 doi:10.1029/2006JD008003, 2007.

578 Flanner, M. G., Zender, C. S., Hess, P. G., Mahowald, N. M., Painter, T. H., Ramanathan, V.,
579 and Rasch, P. J.: Springtime warming and reduced snow cover from carbonaceous particles,
580 Atmos. Chem. Phys., 9, 2481-2497, doi:10.5194/acp-9-2481-2009, 2009.
581 Flanner, M. G., Liu, X., Zhou, C., Penner, J. E., and Jiao, C. (2012), Enhanced solar energy
582 absorption by internally-mixed black carbon in snow grains, Atmos. Chem. Phys., 12,
583 4699-4721, doi:10.5194/acp-12-4699-2012, 2012.
584 Graham, W. F., and Duce, R. A.: The atmospheric transport of phosphorus to the western
585 North‐Atlantic, Atmos. Environ., 16, 1089‐1097, doi:10.1016/0004-6981(82)90198-6,
586 1982.
587 Grell, G., Peckham, S., Schmitz, R., et al.: Fully coupled "online" chemistry within the WRF
588 model, Atmos. Environ., 39(37), 6957–6975, 2005.
589 Griffin, D., and Anchukaitis, K. J.: How unusual is the 2012–2014 California drought?, Geophys.
590 Res. Lett., 41, 9017–9023, doi:10.1002/2014GL062433, 2014.
591 Gu, Y., Liou, K. N., Xue, Y., Mechoso, C. R., Li, W., and Luo, Y.: Climatic effects of different
592 aerosol types in China simulated by the UCLA general circulation model, J. Geophys. Res.,
593 111, D15201, doi:10.1029/2005JD006312, 2006.
594 Gu, Y., Liou, K. N., Jiang, J. H., Su, H., and Liu, X.: Dust aerosol impact on North Africa
595 climate: a GCM investigation of aerosol-cloud-radiation interactions using A-Train satellite
596 data, Atmos. Chem. Phys., 12, 1667-1679, doi:10.5194/acp-12-1667-2012, 2012.
597 Gu, Y., Xue, Y., De Sales, F., and Liou, K. N.: A GCM investigation of dust aerosol impact on
598 the regional climate of North Africa and South/East Asia, Clim. Dyn, 46, 2353-2370, doi
599 10.1007/s00382-015-2706-y, 2016.

600 Gu, Y., Liou, K. N., Jiang, J. H., Fu, R., Lu, S., and Xue, Y.: A GCM investigation of impact of
601 aerosols on the precipitation in Amazon during the dry to wet transition, Clim. Dyn,,
602 48:2393-2404, doi:10.1007/s00382-016-3211-7, 2017.
603 Gustafson, W. I., Chapman, E. G., Ghan, S. J., Easter, R. C., and Fast, J. D.: Impact on modeled
604 cloud characteristics due to simplified treatment of uniform cloud condensation nuclei
605 during NEAQS 2004, Geophys. Res. Lett., 34, L19809, doi:10.1029/2007GL030021, 2007.
606 Hansen, J., Sato, M., and Ruedy, R.: Radiative forcing and climate response, J. Geophys. Res.,
607 102, 6831– 6864, doi:10.1029/96JD03436, 1997.
608 Hadley, O. L., Corrigan, C. E., Kirchstetter, T. W., Cliff, S. S., and Ramanathan, V.: Measured
609 black carbon deposition on the Sierra Nevada snow pack and implication for snow pack
610 retreat, Atmos. Chem. Phys., 10, 7505-7513, doi:10.5194/acp-10-7505-2010, 2010.
611 Hadley, O. L., and Kirchstetter, T. W.: Black-carbon reduction of snow albedo. Nature Climate
612 Change, 2, 437-440, doi:10.1038/nclimate1433, 2012.
613 Hess, M., Koepke, P., and Schult, I.: Optical Properties of Aerosols and Clouds: The Software
614 Package OPAC, Bull. Amer. Meteor. Soc., 79, 831–844,
615 doi:10.1175/15200477(1998)079<0831:OPOAAC>2.0.CO;2, 1998.
616 Hu, Z., C. Zhao, J. Huang, L. R. Leung, Y. Qian, H. Yu, L. Huang, O. V. Kalashnikova (2016):
617 Trans-pacific transport and evolution of aerosols: Evaluation of quasi-global WRF-Chem
618 simulation with multiple observations, Geosci. Model Dev., 9, 1725–1746, 2016.
619 Jacobson, M. Z.: Climate response of fossil fuel and biofuel soot, accounting for soot's feedback
620 to snow and sea ice albedo and emissivity, J. Geophys. Res., 109(D21201),
621 doi:10.1029/2004JD004945, 2004.

622 Jiang, H., and Feingold, G.: Effect of aerosol on warm convective clouds: Aerosol-cloud-surface
623 flux feedbacks in a new coupled large eddy model, J. Geophys. Res., 111, D01202,
624 doi:10.1029/2005JD006138, 2006.
625 Jiang, J.H., Livesey, N.J., Su, H., Neary, L., McConnell, J.C., and Richards, N.A.: Connecting
626 surface emissions, convective uplifting, and long-range transport of carbon monoxide in the
627 upper-troposphere: New observations from the Aura Microwave Limb Sounder, *Geophys.*
628 *Res. Lett.* 34, L18812, doi:10.1029/2007GL030638, 2007.
629 Johnson,J.B.,and Marks, D.:Thedetectionandcorrectionof snow-water equivalent pressure sensor
630 errors, Hydrol. Processes, 18, 3513–3525, 2004.
631 Kiehl, J. and Briegleb, B.: The relative roles of sulfate aerosols and greenhouse gases in climate
632 forcing, Science, 260, 311-314, 1993.
633 Kim, J., Gu, Y., and Liou, K.-N.: The impact of the direct aerosol radiative forcing on surface
634 insolation and spring snowmelt in the southern Sierra Nevada, J. Hydrometeorol., 7, 976-
635 983, 2006.
636 Koren, I., Kaufman, Y. J., Remer, L. A., and Martins, J. V.: Measurement of the effect of
637 Amazon smoke on inhibition of cloud formation, Science, 303, 1342–1345,
638 doi:10.1126/science.1089424, 2004.
639 Lee, W.-L. and Liou, K. N.: Effect of absorbing aerosols on snow albedo reduction in the Sierra
640 Nevada. Atmospheric Environment, 55, 425–430. doi:10.1016/j.atmosenv.2012.03.024,
641 2012.
642 Leung, L. R., Qian, Y., Bian, X., Washington, W. M., Han, J., and Roads, J. O.: Mid-century
643 ensemble regional climate change scenarios for the western United States, Climatic Change,
644 62, 75– 113, 2004.

645 Lynn, B., Khain, A., Rosenfeld, D., and Woodley, W. L.: Effects of aerosols on precipitation
646 from orographic clouds, J. Geophys. Res., 112, D10225, doi:10.1029/2006JD007537, 2007.
647 Mills, M. M., Ridame, C., Davey, M., La Roche, J., and Geider, R. J.: Iron and phosphorus co -
648 limit nitrogen fixation in the eastern tropical North Atlantic, Nature, 429, 292 – 294,
649 doi:10.1038/nature02550, 2004.
650 Oaida, C. M., Xue, Y., Flanner, M. G., Skiles, S. M., De Sales, F., and Painter, T. H.: Improving
651 snow albedo processes in WRF/SSiB regional climate model to assess impact of dust and
652 black carbon in snow on surface energy balance and hydrology over western U.S., J.
653 Geophys. Res. Atmos., 120, 3228–3248. doi: 10.1002/2014JD022444, 2015.
654 Painter, T. H., Barrett, A. P., Landry, C. C., Neff, J. C., Cassidy, M. P., Lawrence, C. R.,
655 McBride, K. E., and Farmer, G. L.: Impact of disturbed desert soils on duration of
656 mountain snow cover, Geophys. Res. Lett., 34, L12502, doi:10.1029/2007GL030284, 2007.
657 Painter, T. H., Deems, J. S., Belnap, J., Hamlet, A. F., Landry, C. C., Udall, B.: Response of
658 Colorado River runoff to dust radiative forcing in snow, Proceedings of the National
659 Academy of Sciences, 2010, 107, 40, 17125, 2010.
660 Platnick, S., and Twomey, S.: Determining the susceptibility of cloud albedo to changes in
661 droplet concentration with the Advanced Very High Resolution Radiometer, J. Appl.
662 Meteor., 33, 334-347, 1994.
663 Qian Y, Leung, L. R., Ghan, S. J., and Giorgi, F.: Regional Climate Effects of Aerosols Over
664 China: Modeling and Observation, Tellus Series B, Chemical and Physical Meteorology
665 55(4):914-934, 2003.
666 Qian, Y., Gustafson Jr., W. I., Leung, L. R., and Ghan, S. J.: Effects of soot-induced snow albedo
667 change on snowpack and hydrological cycle in western United States based on Weather

Research and Forecasting chemistry and regional climate simulations, J. Geophys. Res., 114, D03108, doi:10.1029/2008JD011039, 2009a.

Qian, Y., Gong, D., Fan, J., Leung, L. R., Bennartz, R., Chen, D, and Wang, W.: Heavy pollution suppresses light rain in China: observations and modeling, J. Geophys. Res. D. (Atmospheres) 114:article number D00K02, doi:10.1029/2008JD011575, 2009b.

Qian, Y., Flanner, M. G., Leung, L. Y. R., and Wang, W.: Sensitivity studies on the impacts of Tibetan Plateau snowpack pollution on the Asian hydrological cycle and monsoon climate, Atmos. Chem. Phys., 11(5):1929-1948. doi:10.5194/acp-11-1929-2011, 2011.

Qian, Y., Yasunari, T. J., Doherty, S. J., Flanner, M. G., Lau, W. K., Ming, J., Wang, H., Wang, M., Warren, S. G., and Zhang, R.: Light-absorbing Particles in Snow and Ice: Measurement and Modeling of Climatic and Hydrological Impact, Advances in Atmospheric Sciences 32(1):64-91, doi:10.1007/s00376-014-0010-0, 2015.

Rasmussen, R. M. and Coauthors: Weather Support to Deicing Decision Making (WSDDM): A winter weather nowcasting system, Bull. Amer. Meteor. Soc., 82, 579–595, 2001.

Rosenfeld, D., Woodley, W. L., Axisa, D., Freud, E., Hudson, J. G., and Givati, A.: Aircraft measurements of the impacts of pollution aerosols on clouds and precipitation over the Sierra Nevada, J. Geophys. Res., 113, D15203, doi:10.1029/2007JD009544, 2008a.

Rosenfeld, D., Lohmann, U., Raga, G. B., O'Dowd, C. D., Kulmala, M., Fuzzi, S., Reissell, A., and Andreae, M. O.: Flood or drought: How do aerosols affect precipitation?, Science, 321, 1309–1313, doi:10.1126/science.1160606, 2008b.

Serreze, M. C., Clark, M. P., Armstrong, R. L., McGinnis, D. A., and Pulwarty, R. S.: Characteristics of the western United States snowpack from snowpack telemetry (SNOTEL) data. Water Resour. Res., 35, 2145–2160, 1999.

691 Serreze, M. C., Clark, M. P., and Frei, A.: Characteristics of large snowfall events in the montane
692 western United States as examined using snowpack telemetry (SNOTEL) data. Water
693 Resour. Res., 37, 675–688, 2001.
694 Shindell, D.T., Pechony, O., Voulgarakis, A., Faluvegi, G., Nazarenko, L., Lamarque, J.-F.,
695 Bowman, K., Milly, G., Kovari, B., Ruedy, R., and Schmidt, G.: Interactive ozone and
696 methane chemistry in GISS-E2 historical and future climate simulations. Atmos. Chem.
697 Phys., 13, 2653-2689, doi:10.5194/acp-13-2653-2013, 2013.
698 Sokolik, I. N., Winker, D. M., Bergametti, G., Gillette, D. A., Carmichael, G., Kaufman, Y. J.,
699 Gomes, L., Schuetz, L., and Penner, J. E.: Introduction to special section: Outstanding
700 problems in quantifying the radiative impacts of mineral dust, J. Geophys. Res., 106(D16),
701 18,015 – 18,027, doi:10.1029/2000JD900498, 2001.
702 Toon, O.B., McKay, C.P., Ackerman, T.P. and Santhanam, K.: Rapid calculation of radiative
703 heating rates and photodissociation rates in inhomogeneous multiple scattering
704 atmospheres. Journal of Geophysical Research 94: doi: 10.1029/89JD01321. issn: 0148-
705 0227, 1989.
706 Twomey, S.: The influence of pollution on the shortwave albedo of clouds. J. Atmos. Sci., 34,
707 1149-1152, 1977.
708 VanCuren, R. A.: Asian aerosols in North America: Extracting the chemical composition and
709 mass concentration of the Asian continental aerosol plume from long-term aerosol records
710 in the western United States, J. Geophys. Res., 108, 4623, doi:10.1029/2003JD003459,
711 D20, 2003.
712 VanCuren, R.A., Cliff, S.S., Perry, K.D. and Jimenez-Cruz, M.: Asian continental aerosol
713 persistence above the marine boundary layer over the eastern North Pacific: Continuous

aerosol measurements from Intercontinental Transport and Chemical Transformation 2002 (ITCT 2K2), J. Geophys. Res., 110: doi: 10.1029/2004JD004973, issn: 0148-0227, 2005.

Vicars, W. C., and Sickman, J. O.: Mineral dust transport to the Sierra Nevada, California: Loading rates and potential source areas, J. Geophys. Res., 116, G01018, doi:10.1029/2010JG001394, 2011.

Waliser, D. E., and Coauthors: Simulating the Sierra Nevada snowpack: The impact of snow albedo and multi-layer snow physics, Climatic Change, 109 (Suppl. 1), S95–S117, doi:10.1007/s10584-011-0312-5, 2011.

Wang, Y., Jiang, J. H. and Su, H.: Atmospheric Responses to the Redistribution of Anthropogenic Aerosols, J. Geophys. Res. Atmos., 120, 9625-9641, doi:10.1002/2015JD023665, 2015.

Wang, Y., Wang, M., Zhang, R., Ghan, S.J., Lin, Y., Hu, J., Pan, B., Levy, M., Jiang, J.H., and Molina, M.J.: Assessing the effects of anthropogenic aerosols on Pacific storm track using a multiscale global climate model, Proc. Nat. Acad. Sci. 111, 19, 6894–6899, doi: 10.1073/pnas.1403364111, 2014.

Warren, S., and Wiscombe W.: Dirty snow after nuclear war, Nature, 313, 467–470, 1985.

Wiscombe, W. J. and Warren, S. G.: A model for the spectral albedo of snow, I: Pure snow, J. Atmos. Sci., 37, 2712–2733, 1980.

Wu, L., Su, H., and Jiang, J. H.: Regional simulations of deep convection and biomass burning over South America: 2. Biomass burning aerosol effects on clouds and precipitation, J. Geophys, Res. Atmos., 116, doi:10.1029/2011JD016106, 2011.

735 Wu, L., Su, H., and Jiang, J. H.: Regional simulation of aerosol impacts on precipitation during
736 the East Asian summer monsoon, J. Geophys. Res. Atmos., 118, 6454–6467,
737 doi:10.1002/jgrd.50527, 2013.
738 Wu, L., Su, H., Kalashnikova, O. V., Jiang, J. H., Zhao, C., Garay, M. J., Campbell, J. R., and
739 Yu, N.: WRF-Chem simulation of aerosol seasonal variability in the San Joaquin Valley,
740 Atmos. Chem. Phys., 17, 7291-7309, https://doi.org/10.5194/acp-17-7291-2017, 2017.
741 Xie, S.-P., Kosaka, Y., and Okumura, Y. M. : Distinct energy budgets for anthropogenic and
742 natural changes during global warming hiatus, Nature geoscience, 9, 29-33,
743 doi:10.1038/ngeo2581, 2016.
744 Yang, D., Goodison, B. E., Metcalfe, J. R., Golubev, V. S., Bates, R., Pangburn, T., and Hanson,
745 C. L.: Accuracy of NWS 8'' standard nonrecording precipitation gauge: Results and
746 application of WMO intercomparison. J. Atmos. Oceanic Technol., 15, 54–68, 1998.
747 Zaveri, R. A. and Peters, L. K.: A new lumped structure photochemical mechanism for large-
748 scale applications, J. Geophys. Res., 104, 30387–30415, 1999.
749 Zaveri, R. A., Easter, R. C., Fast, J. D., and Peters, L. K.: Model for Simulating Aerosol
750 Interactions and Chemistry (MOSAIC), J. Geophys. Res., 113, D13204,
751 doi:10.1029/2007JD008782, 2008.
752 Zhao, C., Liu, X., Leung, L. R., Johnson, B., McFarlane, S. A., Gustafson Jr., W. I., Fast, J. D.,
753 and Easter, R.: The spatial distribution of mineral dust and its shortwave radiative forcing
754 over North Africa: modeling sensitivities to dust emissions and aerosol size treatments,
755 Atmos. Chem. Phys., 10, 8821–8838, doi:10.5194/acp-10-8821-2010, 2010.

Zhao, C., Liu, X., Ruby Leung, L., and Hagos, S.: Radiative impact of mineral dust on monsoon precipitation variability over West Africa, Atmos. Chem. Phys., 11, 1879–1893, doi:10.5194/acp11-1879-2011, 2011.

Zhao, C., Leung, L. R., Easter, R., Hand, J., and Avise, J.: Characterization of speciated aerosol direct radiative forcing over California, J. Geophys. Res., 118, 2372–2388, doi:10.1029/2012JD018364, 2013a.

Zhao, C., Chen, S., Leung, L. R., Qian, Y., Kok, J. F., Zaveri, R. A., and Huang, J.: Uncertainty in modeling dust mass balance and radiative forcing from size parameterization, Atmos. Chem. Phys., 13, 10733–10753, doi:10.5194/acp-13-10733-2013, 2013b.

Zhao, C., Hu, Z., Qian, Y., Ruby Leung, L., Huang, J., Huang, M., Jin, J., Flanner, M. G., Zhang, R., Wang, H., Yan, H., Lu, Z., and Streets, D. G.: Simulating black carbon and dust and their radiative forcing in seasonal snow: a case study over North China with field campaign measurements, Atmos. Chem. Phys., 14, 11475-11491, doi:10.5194/acp-14-11475-2014, 2014.

770 **List of Table**

771 Table 1. Model configuration

Atmospheric Process	WRF-Chem option
Microphysics	Morrison double-moment
Radiation	RRTMG for both shortwave and longwave
Land surface	CLM4 with SNICAR included
Planetary boundary layer (PBL)	YSU
Cumulus	No cumulus scheme used
Chemical driver	CBM-Z
Aerosol driver	MOSAIC 4-bin
Anthropogenic emission	NEI05
Biogenic emission	MEGAN
Biomass burning emission	GFEDV2.1
Dust emission	DUSTRAN
Meteorological initial and boundary conditions	ERA-Interim
Chemical initial and boundary conditions	MOZART-4 divided by 2

772

773 Table 2. Experiment design for various aerosol sources.

Experiment	Anthropogenic Aerosols	Dust Aerosol	Transport	Description
CTRL	Y	Y	Y	Control experiment with all aerosol emissions/transports included
NoDust	Y	N	Y	Dust aerosol emission is not included
NoAnth	N	Y	Y	Anthropogenic aerosol emissions are not included
NoTran	Y	Y	N	Aerosol transports are not included
CLEAN	N	N	N	Aerosol emissions/transports are not included

774

775 Table 3. Experiment design for various aerosol pathways.

Experiment	ARI	ACI	ASI	Description
NARI	N	Y	Y	ARI is not included
NASI	Y	Y	N	ASI is not included
NARS	N	Y	N	ARI and ASI are not included

776

Atmos. Chem. Phys. Discuss., https://doi.org/10.5194/acp-2017-597
Manuscript under review for journal Atmos. Chem. Phys.
Discussion started: 24 October 2017

Atmospheric Chemistry and Physics Discussions

777 Table 4. Changes in surface temperature (K) and precipitation, SWE, and surface runoff in
778 percentage averaged over October 2012 to June 2013 due to overall and various aerosol effects
779 for the whole domain (34-42 °N, 117-124 °W, not including ocean points), mountain tops (with
780 elevation ≥ 2.5 km), and lower elevations (< 2.5 km). Total impacts for the simulations from
781 October 2013 to June 2014 are also included as "Total_13-14".

Region	Source/ pathway	T2 (K)	Precipitation (%)	SWE (%)	Surface runoff (%)
Whole Domain	Total	–0.19	–6.87	–3.17	–6.58
	Total_13-14	–0.21	–5.99	–8.88	–5.13
	ARI	–0.14	–0.47	1.88	–0.21
	ASI	0.01	–0.03	–1.96	0.04
	ACI	–0.06	–6.26	–2.67	–6.30
	Anth	–0.02	–1.02	–0.91	–0.94
	Dust	0.00	–0.19	–1.35	0.01
	Tran	–0.17	–2.97	1.89	–2.90
Mountain Tops	Total	0.22	–11.53	–10.50	–9.58
	Total_13-14	0.15	–9.90	–15.57	–3.55
	ARI	–0.09	–0.61	0.76	–0.49
	ASI	0.12	0.26	–3.94	1.10
	ACI	0.17	–11.03	–7.57	–10.25
	Anth	0.03	–1.75	–1.60	–2.06
	Dust	0.10	0.31	–2.99	1.49
	Tran	–0.02	–5.25	–2.43	–4.76
Lower Elevations	Total	–0.21	–6.62	0.42	–6.42
	Total_13-14	–0.22	–5.75	2.66	–5.26
	ARI	–0.14	–0.46	2.43	–0.19
	ASI	0.00	–0.04	–0.99	–0.01
	ACI	–0.07	–6.00	–0.27	–6.09
	Anth	–0.03	–0.98	–0.57	–0.89
	Dust	0.00	–0.22	–0.55	–0.07
	Tran	–0.17	–2.85	4.01	–2.81

782

Atmos. Chem. Phys. Discuss., https://doi.org/10.5194/acp-2017-597
Manuscript under review for journal Atmos. Chem. Phys.
Discussion started: 24 October 2017

Atmospheric Chemistry and Physics Discussions

783 **List of Figures**

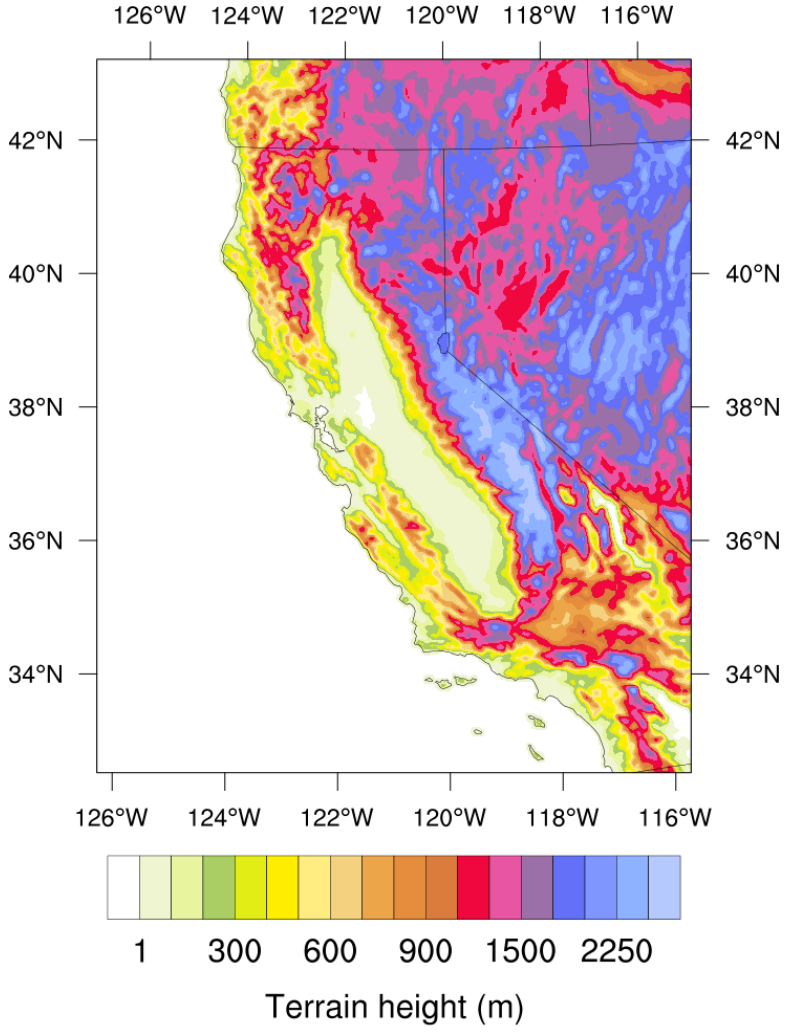

784

785 Figure 1. Model domain and terrain height (m).

Atmos. Chem. Phys. Discuss., https://doi.org/10.5194/acp-2017-597
Manuscript under review for journal Atmos. Chem. Phys.
Discussion started: 24 October 2017

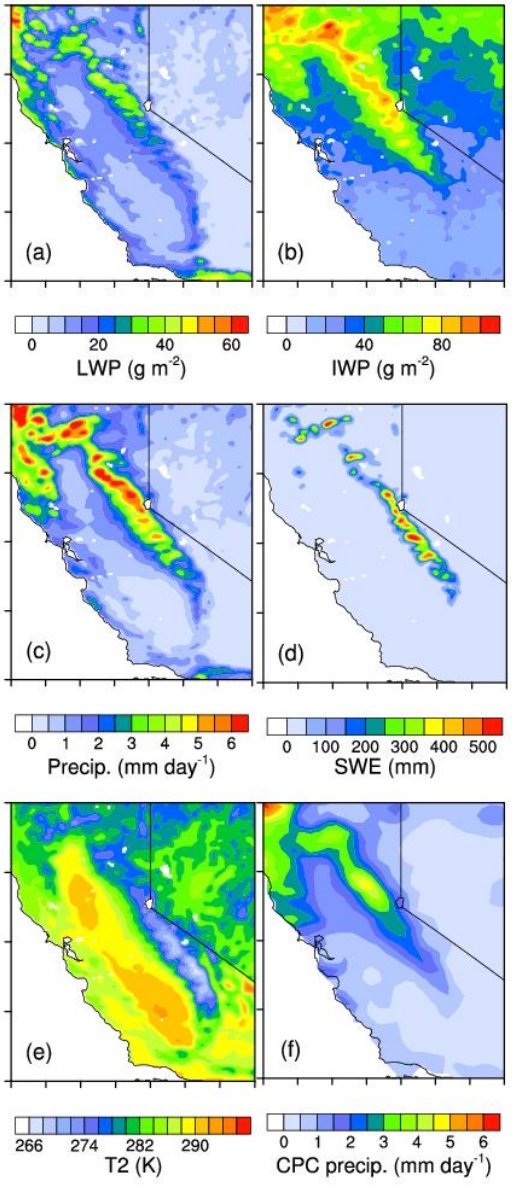

786

787 Figure 2. Model simulated (a) LWP (g m^{-2}), (b) IWP (g m^{-2}), (c) precipitation (mm day^{-1}), (d)
788 SWE (mm), and (e) temperature at 2 meters, T2 (K) from experiment CTRL, and (f) CPC
789 observed precipitation (mm day^{-1}), averaged over October 2012 to June 2013.

Atmos. Chem. Phys. Discuss., https://doi.org/10.5194/acp-2017-597
Manuscript under review for journal Atmos. Chem. Phys.
Discussion started: 24 October 2017

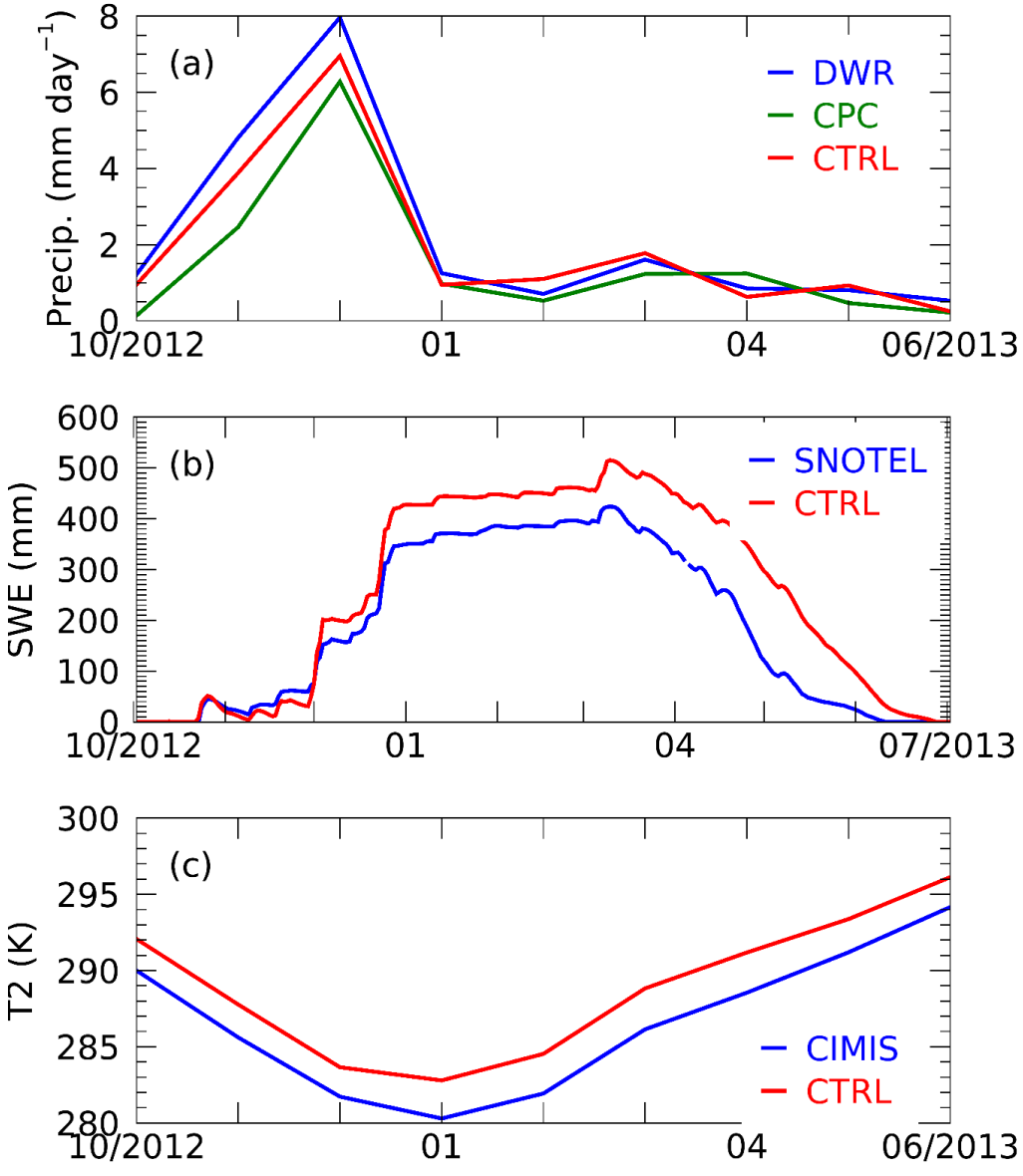

Figure 3. (a) Monthly mean precipitation (mm day^{-1}) simulated from CTRL (red curve) and the observations from CPC (green) and DWR (blue); (b) Daily mean SWE (mm) simulated from CTRL (red) and observed at SNOTEL stations (blue); and (c) Monthly mean T2 (K) simulated from CTRL (red) and the observations from CIMIS (blue).

Atmos. Chem. Phys. Discuss., https://doi.org/10.5194/acp-2017-597
Manuscript under review for journal Atmos. Chem. Phys.
Discussion started: 24 October 2017

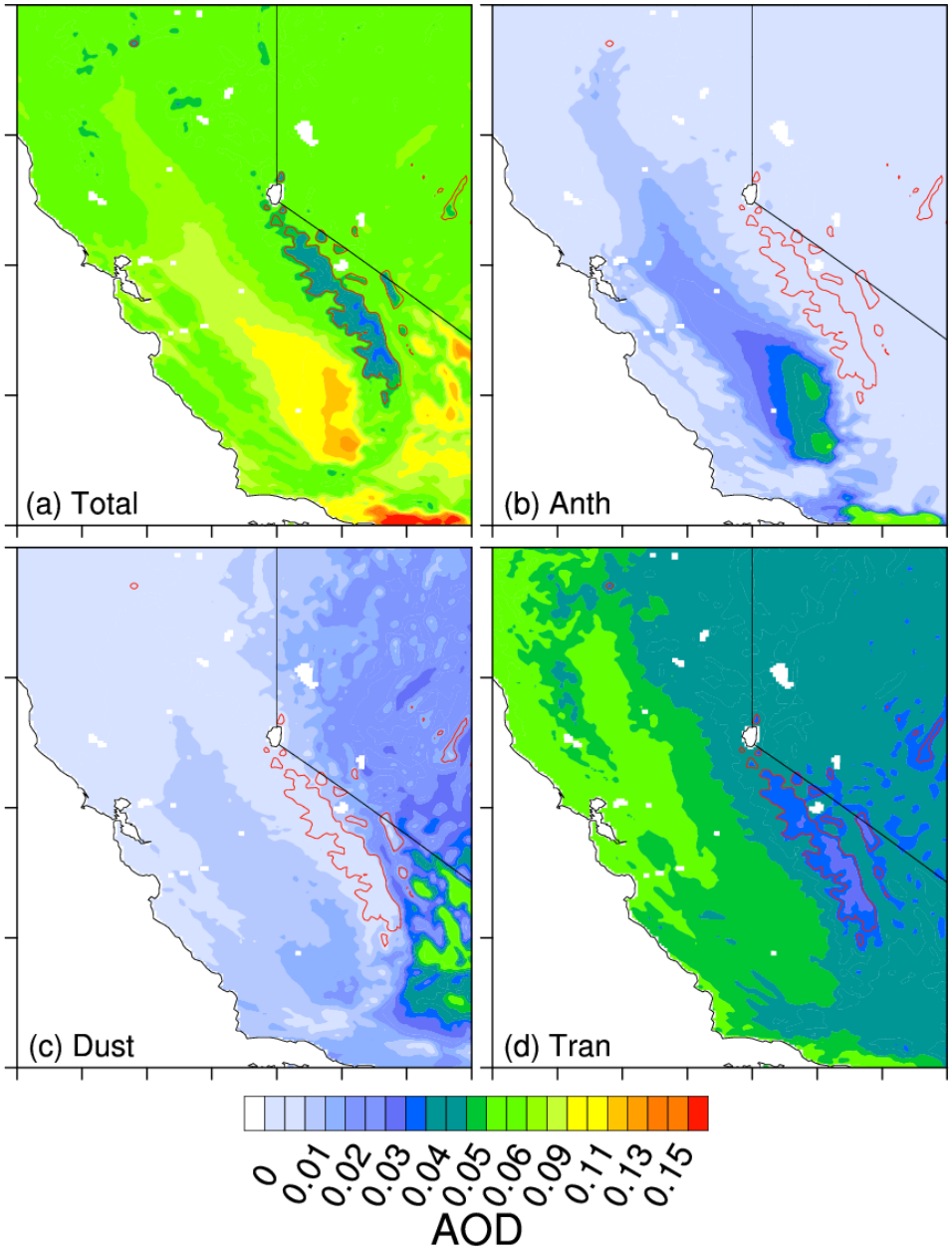

795

796 Figure 4. Spatial distribution of aerosol optical depth (AOD) for (a) all aerosols, (b) local
797 anthropogenic aerosols, (c) local dust aerosols, and (d) transported aerosols from outside the
798 domain, simulated from CTRL. Red lines represent the mountain tops with elevation ≥ 2.5 km.

Atmos. Chem. Phys. Discuss., https://doi.org/10.5194/acp-2017-597
Manuscript under review for journal Atmos. Chem. Phys.
Discussion started: 24 October 2017

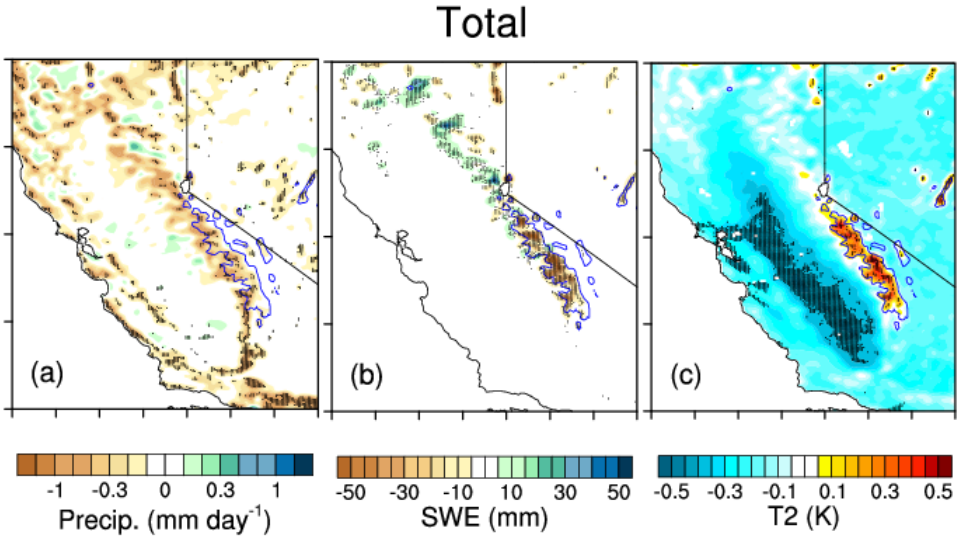

799

800 Figure 5. Total aerosol effects (CTRL – CLEAN) on spatial distribution of (a) precipitation (mm
801 day^{-1}), (b) SWE (mm), and (c) T2 (K). The dotted area denotes statistical significance above the
802 90% confidence level. Blue lines represent the mountain tops with elevation $\geq$ 2.5 km.

Atmos. Chem. Phys. Discuss., https://doi.org/10.5194/acp-2017-597
Manuscript under review for journal Atmos. Chem. Phys.
Discussion started: 24 October 2017

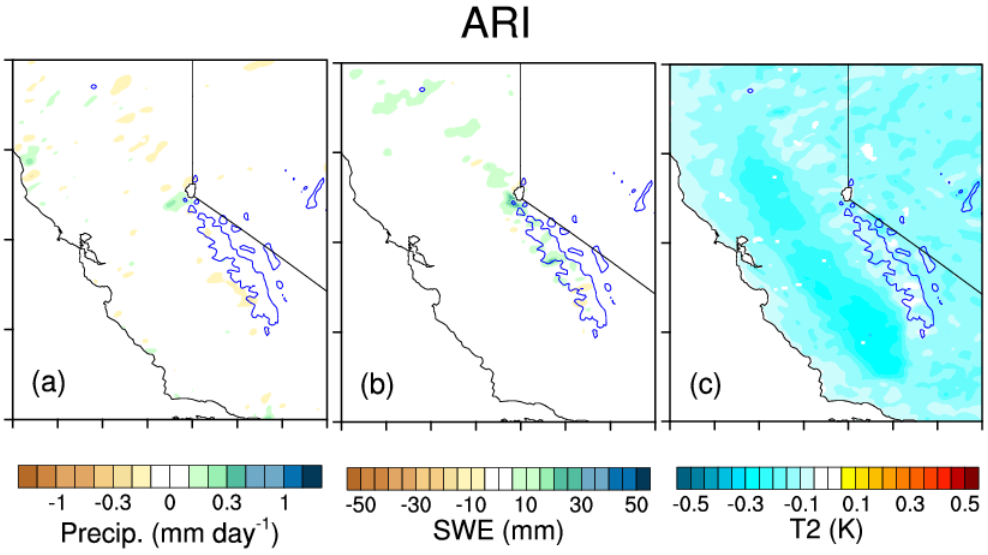

803

804 Figure 6. ARI effects (CTRL – NARI) on spatial distribution of (a) precipitation (mm day^{-1}), (b)

805 SWE (mm), and (c) T2 (K). Blue lines represent the mountain tops with elevation ≥ 2.5 km.

Atmos. Chem. Phys. Discuss., https://doi.org/10.5194/acp-2017-597
Manuscript under review for journal Atmos. Chem. Phys.
Discussion started: 24 October 2017

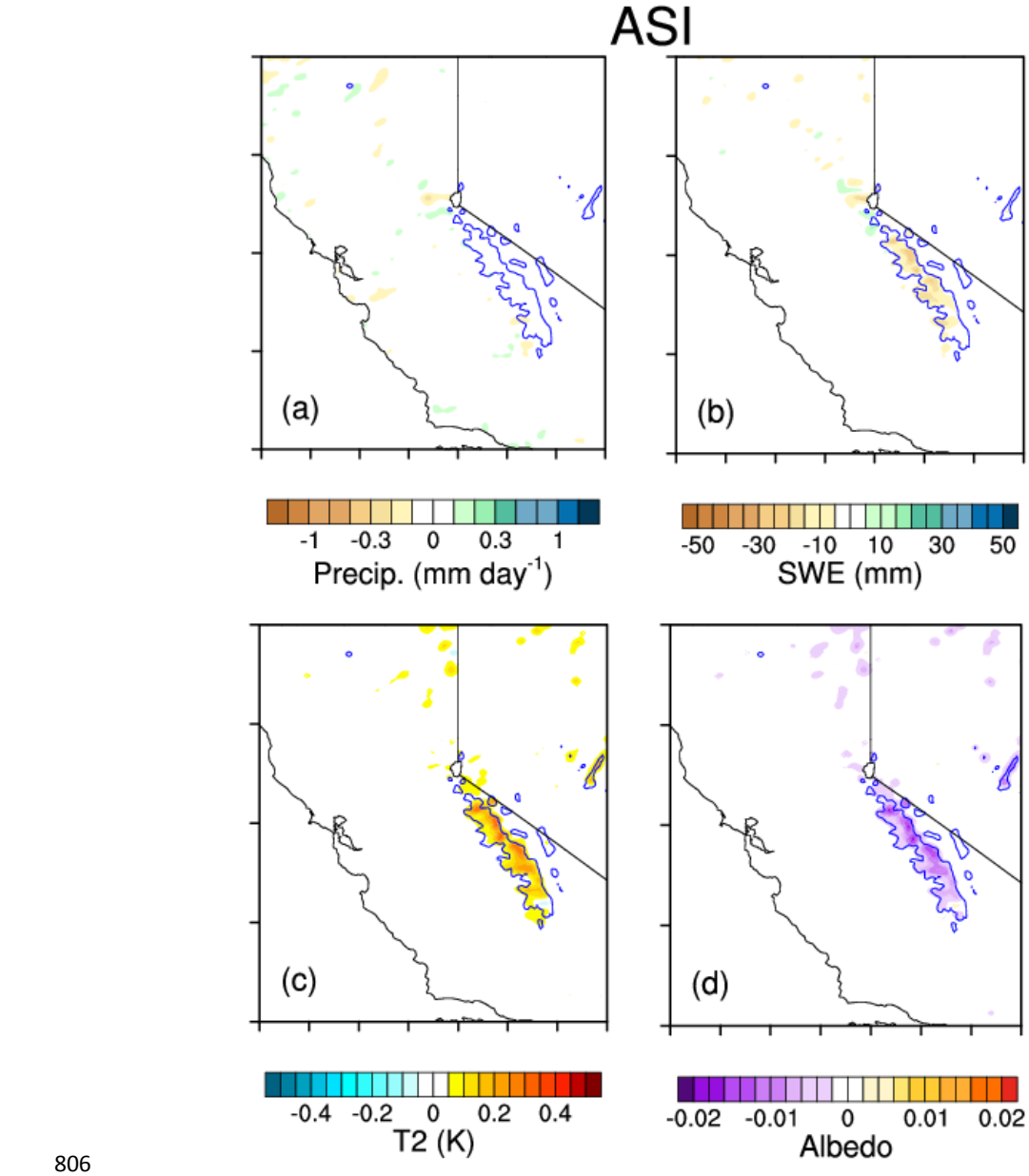

806

807 Figure 7. ASI effects (CTRL – NASI) on spatial distribution of (a) precipitation (mm day^{-1}), (b)
808 SWE (mm), (c) T2 (K), and (d) surface albedo. Blue lines represent the mountain tops with
809 elevation ≥ 2.5 km.

Atmos. Chem. Phys. Discuss., https://doi.org/10.5194/acp-2017-597
Manuscript under review for journal Atmos. Chem. Phys.
Discussion started: 24 October 2017

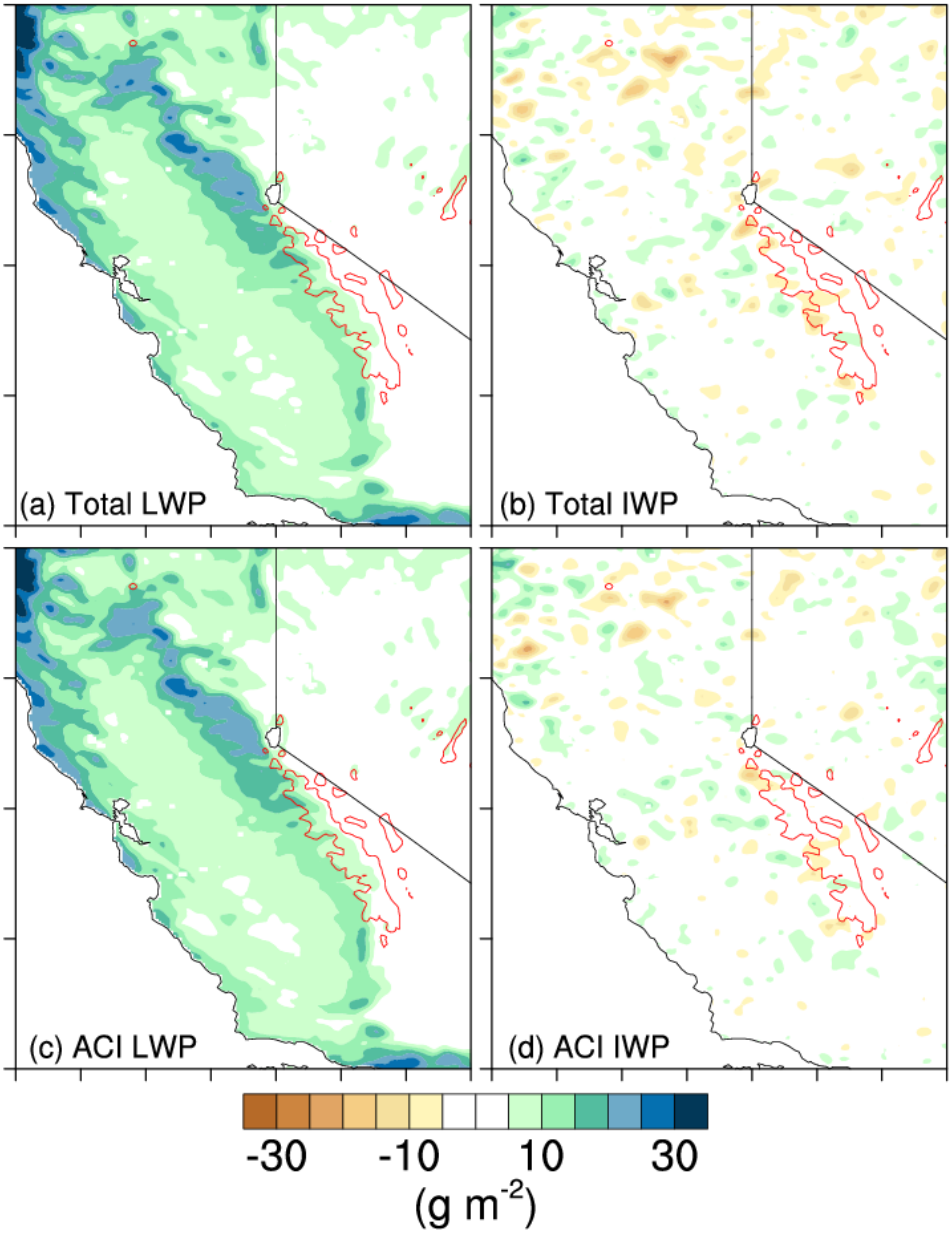

Figure 8. Differences in (a) LWP (g m^{-2}) and (b) IWP (g m^{-2}) due to all aerosol effects (CTRL – CLEAN), and (c) LWP (g m^{-2}) and (d) IWP (g m^{-2}) due to ACI effect (NARS – CLEAN). Red lines represent the mountain tops with elevation ≥ 2.5 km.

Atmos. Chem. Phys. Discuss., https://doi.org/10.5194/acp-2017-597
Manuscript under review for journal Atmos. Chem. Phys.
Discussion started: 24 October 2017

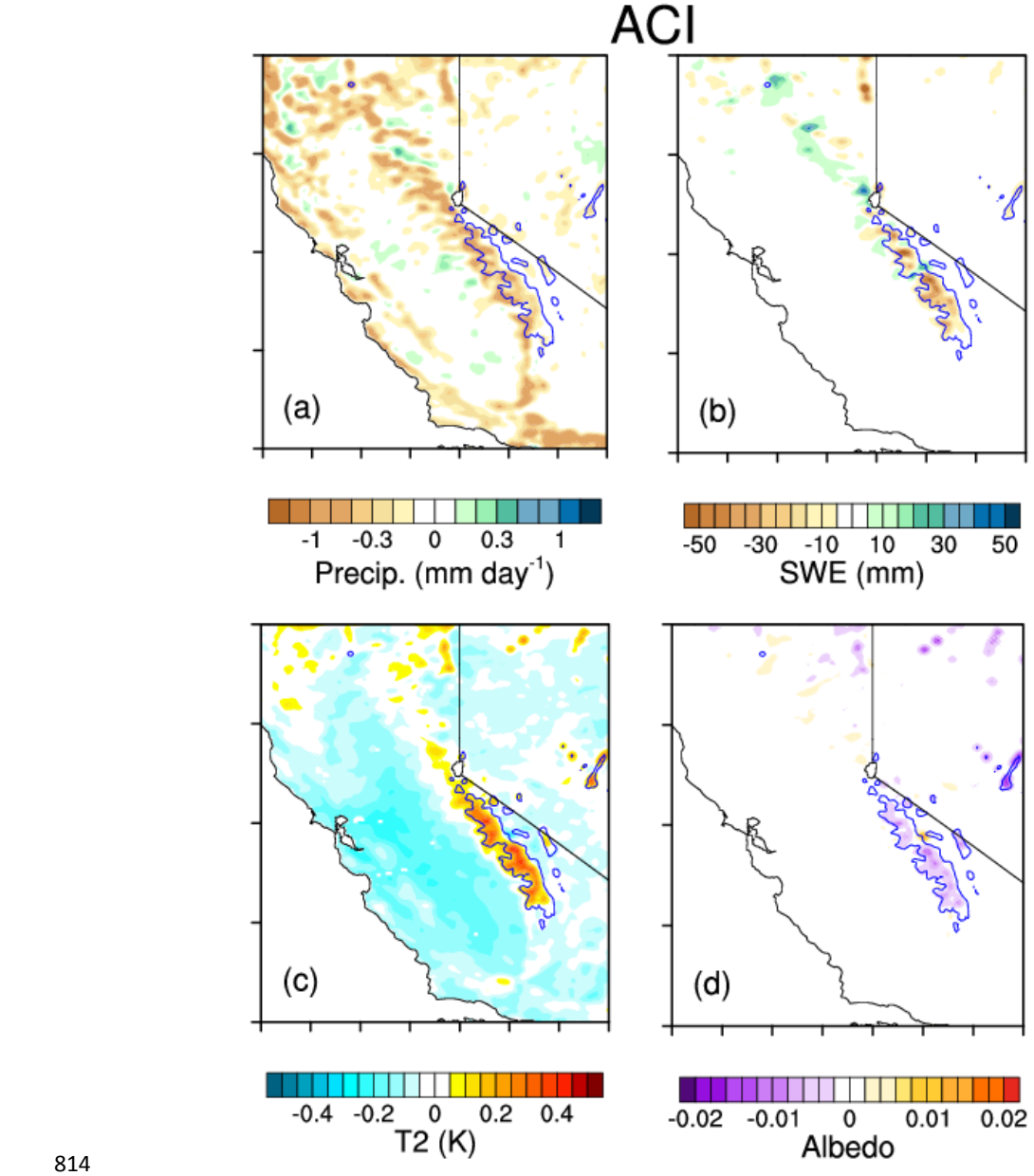

814

815 Figure 9. Same as Figure 7, but for ACI effect (NARS – CLEAN).

Atmos. Chem. Phys. Discuss., https://doi.org/10.5194/acp-2017-597
Manuscript under review for journal Atmos. Chem. Phys.
Discussion started: 24 October 2017

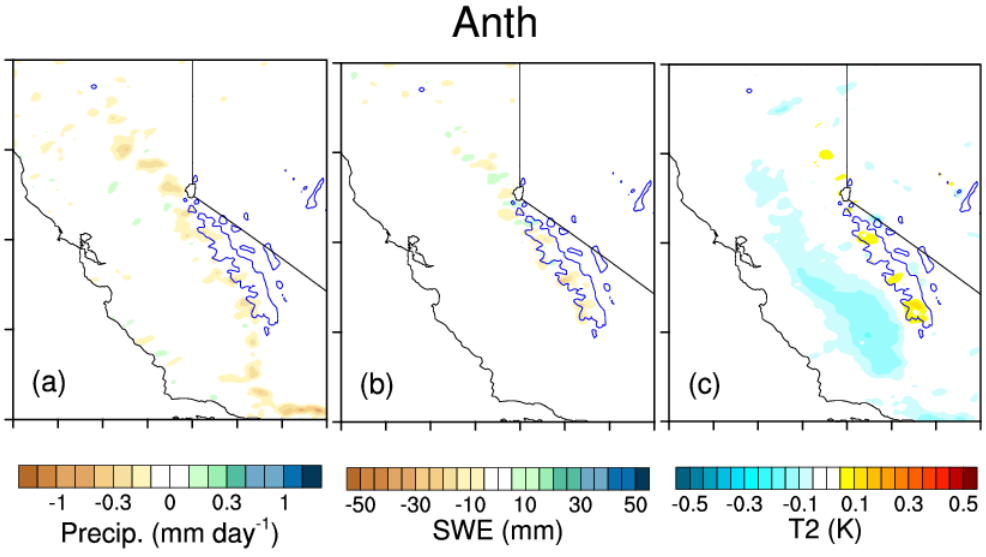

816

817 Figure 10. Effect of local anthropogenic aerosols (CTRL – NoAnth) on spatial distribution of (a)
818 precipitation (mm day^{-1}), (b) SWE (mm), and (c) T2 (K). Blue lines represent the mountain tops
819 with elevation $\geq$ 2.5 km.

Atmos. Chem. Phys. Discuss., https://doi.org/10.5194/acp-2017-597
Manuscript under review for journal Atmos. Chem. Phys.
Discussion started: 24 October 2017

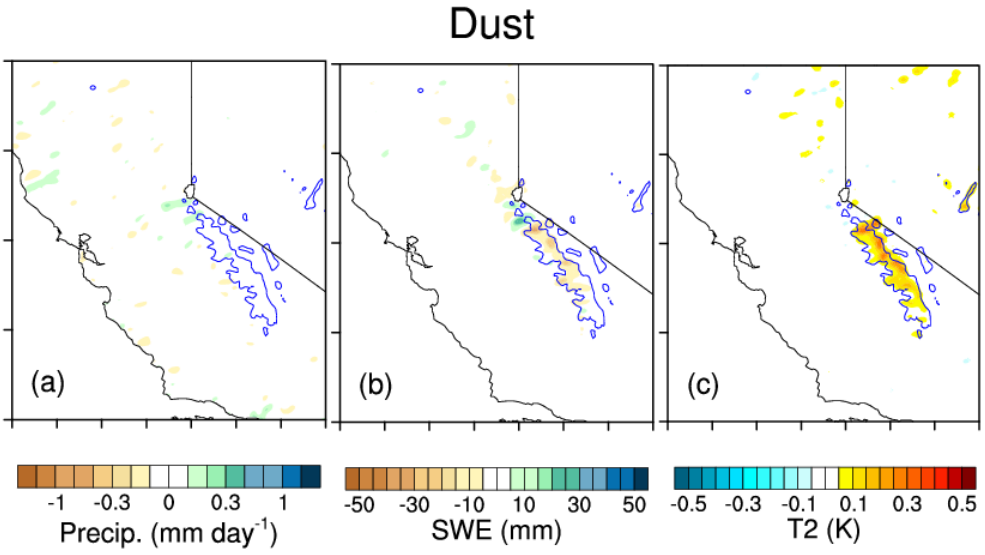

820

821 Figure 11. Same as Figure 10, but for the effect of local dust aerosols (CTRL – NoDust).

Atmos. Chem. Phys. Discuss., https://doi.org/10.5194/acp-2017-597
Manuscript under review for journal Atmos. Chem. Phys.
Discussion started: 24 October 2017

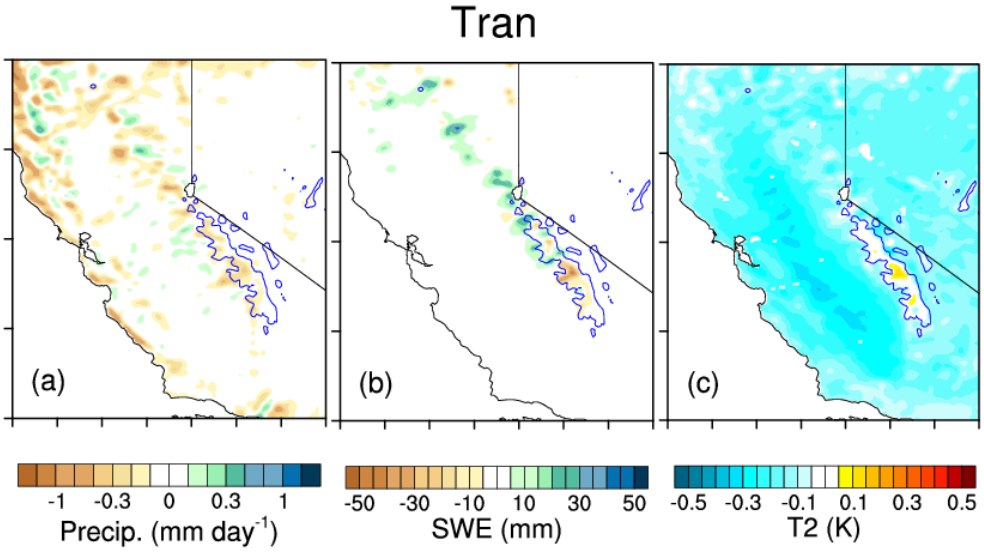

822

823 Figure 12. Same as Figure 10, but for the effect of transported aerosols (CTRL – NoTran).

Atmos. Chem. Phys. Discuss., https://doi.org/10.5194/acp-2017-597
Manuscript under review for journal Atmos. Chem. Phys.
Discussion started: 24 October 2017

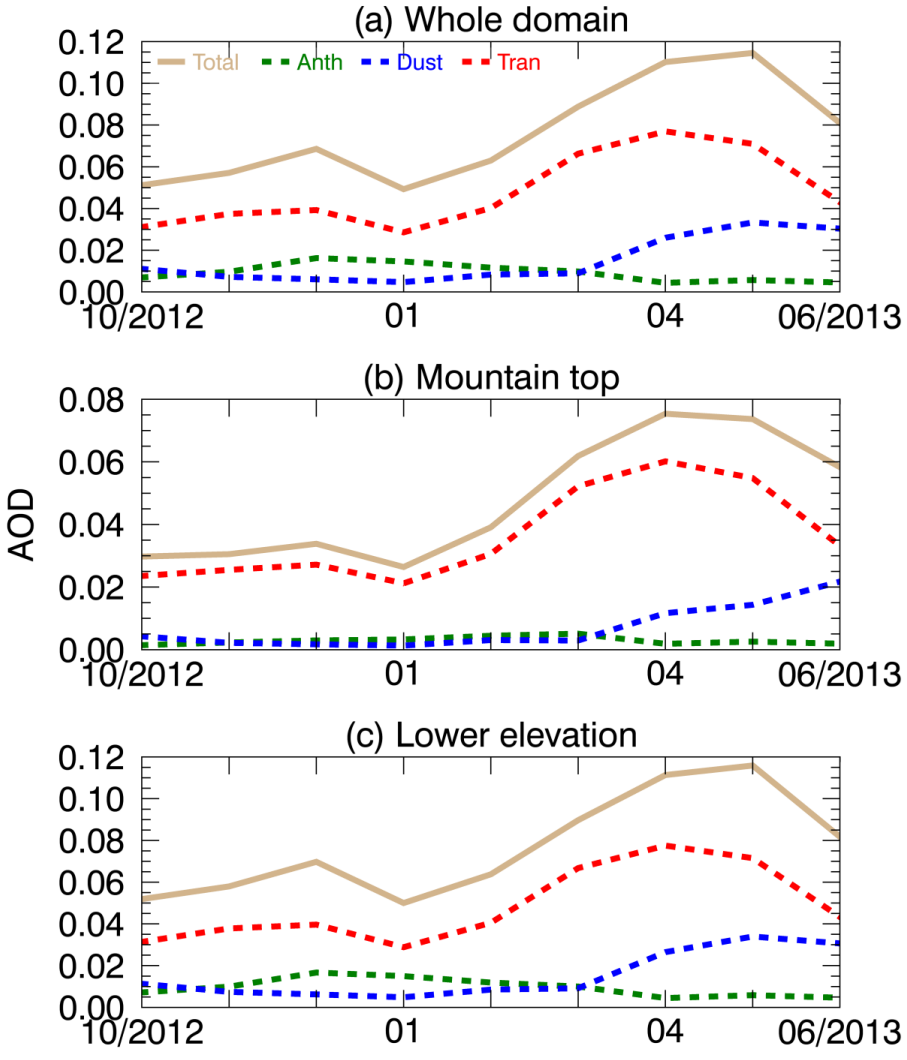

824

825 Figure 13. Monthly mean AOD simulated from CTRL for total aerosols (brown solid), local
826 anthropocentric aerosols (green dashed), local dust (blue dashed), and transported aerosols (red
827 dashed) averaged over (a) the whole domain (34-42 °N, 117-124 °W, not including ocean points),
828 (b) mountain tops (with elevation ≥ 2.5 km), and (c) lower elevation area (< 2.5 km) from
829 October 2012 to June 2013.

Atmos. Chem. Phys. Discuss., https://doi.org/10.5194/acp-2017-597
Manuscript under review for journal Atmos. Chem. Phys.
Discussion started: 24 October 2017

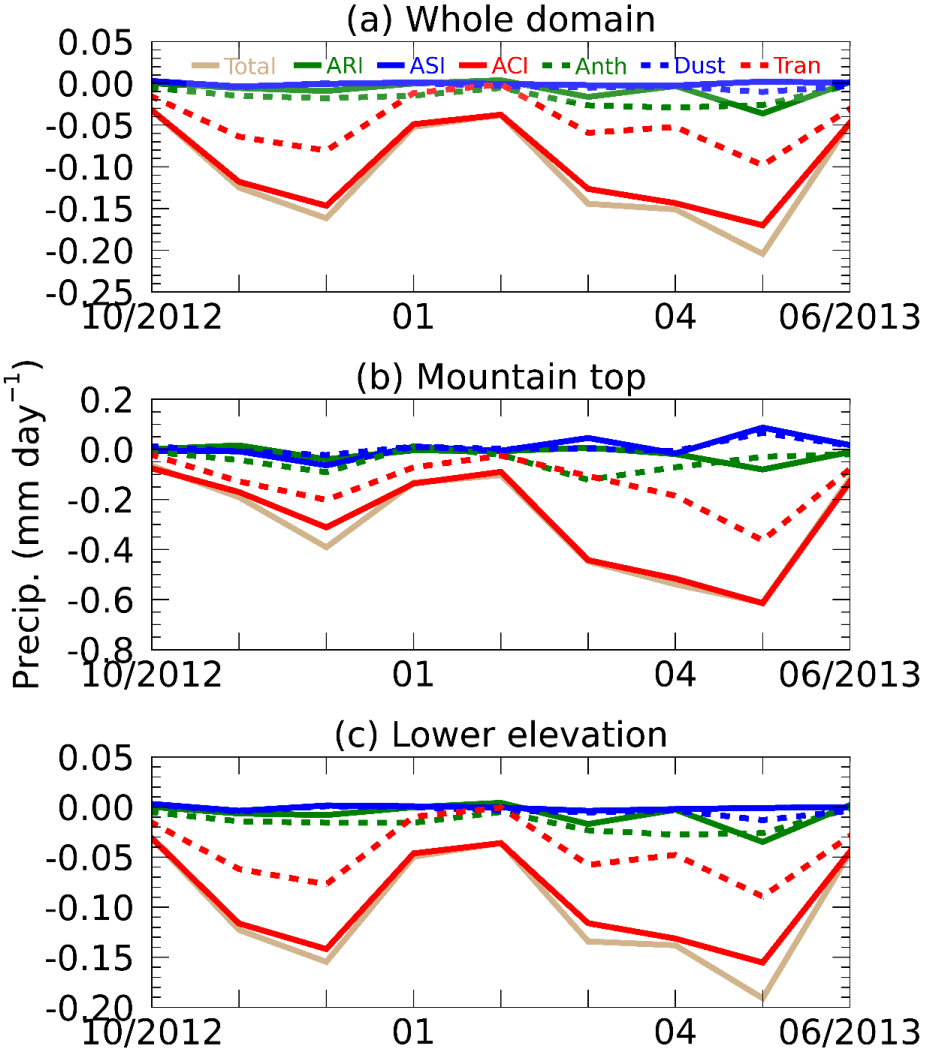

Figure 14. Monthly mean differences in precipitation (mm day^{-1}) due to total aerosols (brown solid), ARI (green solid), ASI (blue solid), ACI (red solid), local anthropocentric aerosols (green dashed), local dust (blue dashed), and transported aerosols (red dashed) averaged over (a) the whole domain (34-42 °N, 117-124 °W, not including ocean points), (b) mountain tops (with elevation $\geq$ 2.5 km), and (c) lower elevation area (< 2.5 km) from October 2012 to June 2013.

Atmos. Chem. Phys. Discuss., https://doi.org/10.5194/acp-2017-597
Manuscript under review for journal Atmos. Chem. Phys.
Discussion started: 24 October 2017

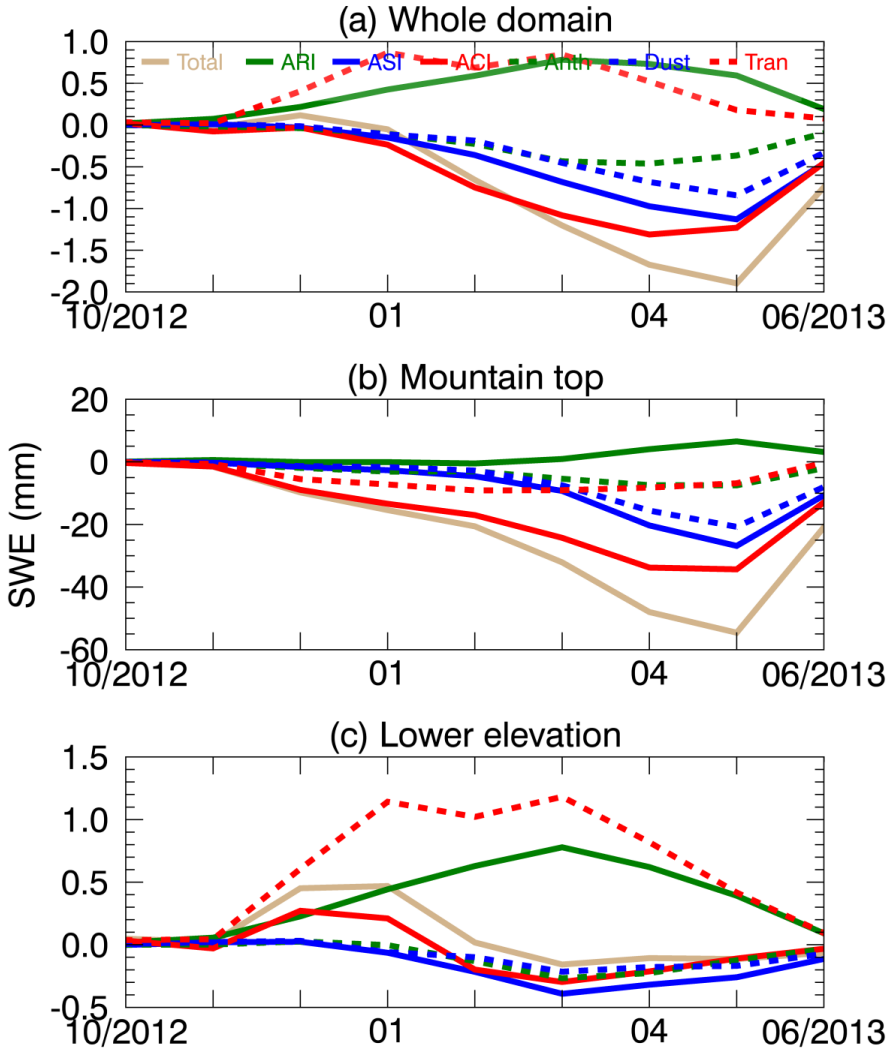

836

837 Figure 15. Same as Figure 14, but for SWE (mm).

Atmos. Chem. Phys. Discuss., https://doi.org/10.5194/acp-2017-597
Manuscript under review for journal Atmos. Chem. Phys.
Discussion started: 24 October 2017

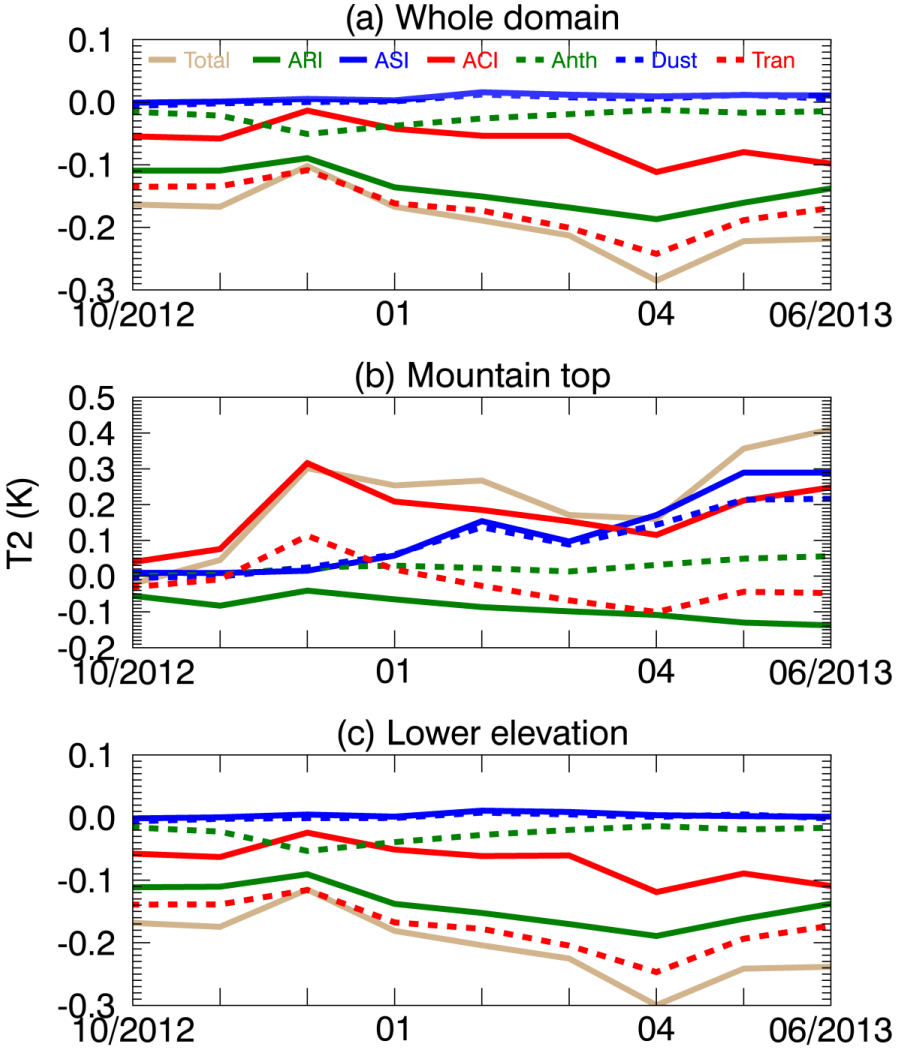

838

839 Figure 16. Same as Figure 14, but for T2 (K).

Atmos. Chem. Phys. Discuss., https://doi.org/10.5194/acp-2017-597
Manuscript under review for journal Atmos. Chem. Phys.
Discussion started: 24 October 2017

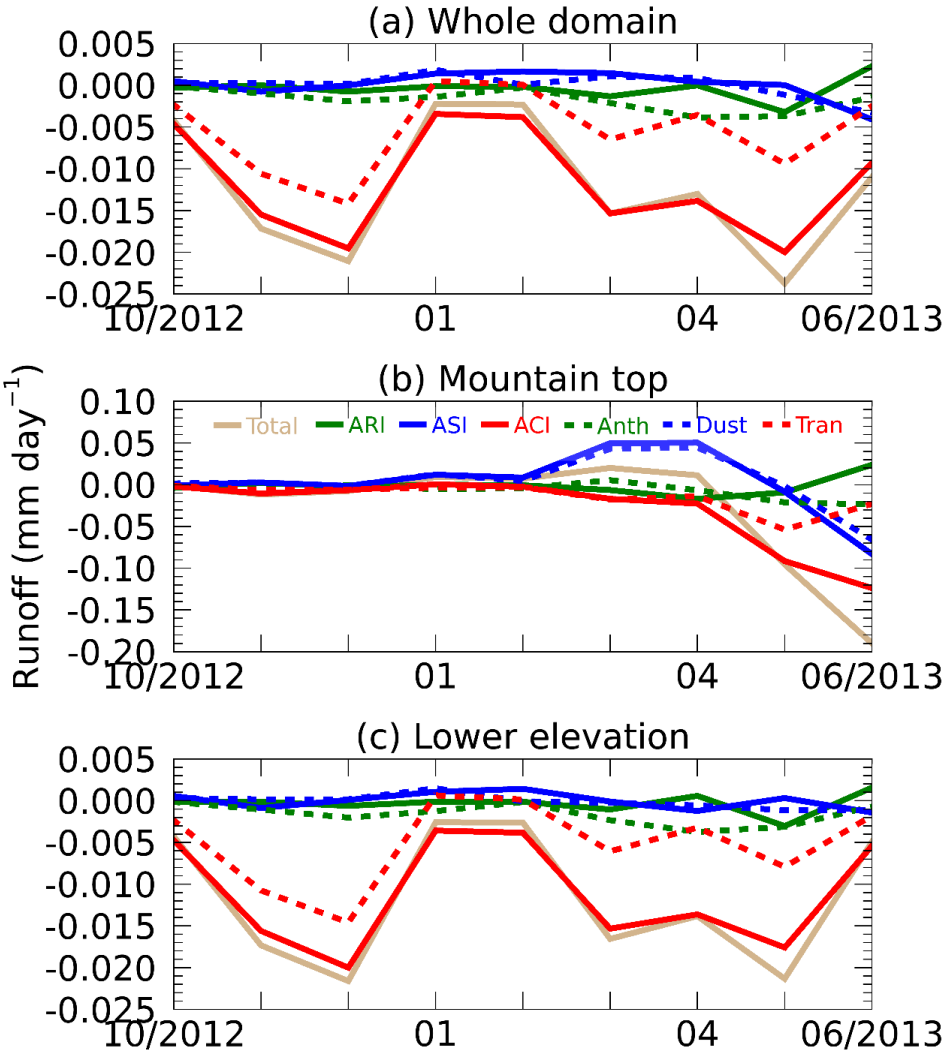

Figure 17. Same as Figure 14, but for surface runoff (mm day^{-1}).